

University of Windsor

Scholarship at UWindor

Electronic Theses and Dissertations

Theses, Dissertations, and Major Papers

2010

The Effects of Cell Surface Proteins and Redox State on Platelet Aggregation and Adhesion

Rebecca Heeney
University of Windsor

Follow this and additional works at: <https://scholar.uwindsor.ca/etd>

Recommended Citation

Heeney, Rebecca, "The Effects of Cell Surface Proteins and Redox State on Platelet Aggregation and Adhesion" (2010). *Electronic Theses and Dissertations*. 304.
<https://scholar.uwindsor.ca/etd/304>

This online database contains the full-text of PhD dissertations and Masters' theses of University of Windsor students from 1954 forward. These documents are made available for personal study and research purposes only, in accordance with the Canadian Copyright Act and the Creative Commons license—CC BY-NC-ND (Attribution, Non-Commercial, No Derivative Works). Under this license, works must always be attributed to the copyright holder (original author), cannot be used for any commercial purposes, and may not be altered. Any other use would require the permission of the copyright holder. Students may inquire about withdrawing their dissertation and/or thesis from this database. For additional inquiries, please contact the repository administrator via email (scholarship@uwindsor.ca) or by telephone at 519-253-3000ext. 3208.

**The Effects of Cell Surface Proteins and Redox State on
Platelet Aggregation and Adhesion**

By

Rebecca C. Heeney

A Thesis

Submitted to the Faculty of Graduate Studies
Through the Department of Chemistry and Biochemistry
In Partial Fulfillment of the Requirements for
The Degree of Master of Science at
The University of Windsor

Windsor, Ontario, Canada

2009

©2009 Rebecca Heeney

**The Effects of Cell Surface Proteins and Redox State on Platelet Aggregation
and Adhesion**

By

Rebecca C. Heeney

APPROVED BY

Dr. J. Hudson
Department of Biological Sciences

Dr. P. Vacratsis
Department of Chemistry and Biochemistry

Dr B. Mutus
Department of Chemistry and Biochemistry

Dr Siryam Pandey, Chair of Defense
Department of Chemistry and Biochemistry

AUTHOR'S DECLARATION OF ORIGINALITY

I hereby certify that I am the sole author of this thesis and that no part of this thesis has been published or submitted for publication.

I certify that, to the best of my knowledge, my thesis does not infringe upon anyone's copyright nor violate any proprietary rights and that any ideas, techniques, quotations, or any other material from the work of other people included in my thesis, published or otherwise, are fully acknowledged in accordance with the standard referencing practices. Furthermore, to the extent that I have included copyrighted material that surpasses the bounds of fair dealing within the meaning of the Canada Copyright Act, I certify that I have obtained a written permission from the copyright owner(s) to include such material(s) in my thesis and have included copies of such copyright clearances to my appendix.

I declare that this is a true copy of my thesis, including any final revisions, as approved by my thesis committee and the Graduate Studies office, and that this thesis has not been submitted for a higher degree to any other University or Institution.

ABSTRACT

Platelet aggregation is a complex process that results in side effects for patients with diabetes, atherosclerosis, stroke and heart attack. Although thoroughly studied, the details of the aggregation cascade are not determined. The mechanism for participation of protein disulfide isomerase (PDI) in platelet function has received attention in literature however has not been established. In addition, heat shock protein 70 (Hsp70) was found on the platelet surface and was investigated for its role in platelet aggregation. Thymosin β_4 was of interest as a potential effector in platelet aggregation. An additional goal of the study was further optimization of the flow cell chamber platelet aggregation model.

UV-VIS Spectrophotometric and flow cell chamber data that indicate no significant effect of excess platelet surface PDI, **b-b'** or Hsp70 on platelet aggregation and adhesion. However, Thymosin β_4 has been shown to positively affect rates of platelet aggregation at the doses of 1-10 $\mu\text{g/mL}$.

This work is dedicated to my parents, for their unconditional love,
support and encouragement; and to the love of my life, Lance, for his love
and endless understanding.

ACKNOWLEDGEMENTS

First, I would like to thank my supervisor Dr. Mutus for his ideas, guidance and for welcoming me into his lab. I would also like to thank my committee members Dr. Panayiotis Vacratsis and Dr. John Hudson for their assistance, their ideas and their time.

I would like to acknowledge and thank my labmates and friends, Suzie Durocher and Vasantha Kallakunta. Your presence as sounding boards, a support structure and helping hand have been instrumental in the completion of this thesis.

To my labmates Adam Faccenda, Harman Dhaliwal and Ruchi Chaube, and all of the 4th year and summer students that helped along the way especially Anna Guo, thank you very much for your help and assistance throughout this journey, and may you enjoy many successes.

I would also like to acknowledge and thank my family for their love, support and encouragement during the writing of this thesis.

TABLE OF CONTENTS

AUTHOR’S DECLARATION OF ORIGINALITY	iii
ABSTRACT.....	iv
ACKNOWLEDGEMENTS.....	vi
FIGURE LEGEND	xii
Chapter 1 GENERAL INTRODUCTION	1
1.1 Platelets.....	1
1.1.1 Introduction	1
1.1.2 Platelet Formation.....	1
1.1.3 Platelet Activation	5
1.1.4 Thrombin Activation	5
1.1.5 Integrin Activation.....	6
1.1.6 Heat Shock Protein 70 on the Platelet Surface	10
1.2 Protein Disulfide Isomerase	11
1.2.1 Introduction	11
1.2.2 Domain Structure and Catalytic Activity	11
1.2.3 PDI in Platelet Aggregation.....	16
1.2.4 PDI in Other Roles	19
1.3 Flow Cell Methodology Development.....	20
1.3.1 Introduction	20

1.3.2 Surface Chemistry	21
1.4 Thymosin Beta Four.....	23
1.4.1 Introduction	23
1.4.2 Domain Structure and Activity.....	23
OBJECTIVES	27
Chapter 2 MATERIALS AND METHODS	28
2.1 Materials.....	28
2.2 Methods.....	29
2.2.1 Blood Acquisition.....	29
2.2.2 Platelet Isolation and Preparation.....	29
2.2.3 Cloning of Hsp70.....	30
2.2.4 Protein Purification.....	30
2.2.5 Protein Disulfide Isomerase Preparation: oxidation, reduction and isomerization	31
2.2.6 Spectrophotometer Turbidity Assay Experimental Procedure	32
2.2.7 Flow Chamber Assembly	32
2.2.8 Flow Chamber Experimental Procedure.....	33
2.2.9 Thymosin β_4 Fibrinogen Binding Assay	35
2.2.10 5,5'-Dithiobis(2-nitrobenzoic acid) Assay.....	35
2.2.11 Data Analysis.....	36

Chapter 3 RESULTS.....	37
3.1 Flow Cell Methodology	37
3.1.1 Optimizing the Surface Chemistry	37
3.1.2 Labeling Platelets for Use in Flow Cell Experiments	41
3.2 Excess platelet surface proteins.....	46
3.2.1 Investigation into the role of excess PDI on the platelet surface.....	48
3.2.1.1 Turbidity Assay.....	51
3.2.1.2 Aggregations Under Flow.....	54
3.2.2 Investigation into the role of excess b-b' subunit of PDI on the platelet surface	60
3.2.2.1 Turbidity Assay.....	60
3.2.2.3 Aggregations Under Flow.....	62
3.2.3 Hsp70 and its effects on platelet aggregation.....	64
3.2.3.1 The Effect of Hsp70 on platelet aggregation and adhesion under flow conditions.....	64
3.3 Thymosin Beta Four.....	68
3.3.1 Turbidity Assay	68
3.3.2 The effect of T β_4 on platelet adhesion under flow conditions.....	70
3.3.3 Fibrinogen Binding of T β_4	72
Chapter 4 DISCUSSION	75
4.1 Flow Cell Methodology Development.....	75

4.2 Surface deposition of b-b', PDI and Hsp70 and their effect on platelet aggregation	78
4.3 Thymosin β_4	79
4.4 Future Directions.....	85
REFERENCES	87
VITA AUCTORIS	93

FIGURE LEGEND

Figure 1-1 Megakaryocyte platelet biogenesis (2).....	4
Figure 1-2: Downstream targets and effectors following proteolysis of PAR-1 by thrombin in platelet aggregation.	7
Figure 1-3. Integrin $\alpha_{2b} \beta_3$ extracellular domain structure and affinity states (10). When in the bent conformation the integrin assumes a low affinity state; as it moves from the extended closed conformation to the extended open conformation, the affinity increases achieving the extended open conformation once bound to fibrinogen. In inside-out signaling, interactions between the lower legs are disrupted, initiating the switchblade unfolding of the integrin.	8
Figure 1-4 The a and b domains of human PDI. The a domain contains five-stranded mixed b-sheets surrounded by four a-helices. The active site motif lies between C36 and C39 at the N-terminus of a2. There is virtually no sequence similarity between the domains (32)	13
Figure 1-5 The redox-dependent activities of PDI. By forming mixed disulfides with cysteine residues, PDI is able to form and break disulfide bonds producing a protein with free thiols, disulfide bonds or shuffled disulfide bonds.....	14
Figure 1-6 A model of the proposed disulfide bond shuffle that occurs in integrins on the platelet surface. Resting and active integrins differ in the number and positioning of unpaired cysteines (44).	18
Figure 1-7 The surface chemistry of PDMS flow cells for immobilization of proteins. Plasma oxidation exposes hydroxyl groups on the PDMS surface that are bound by APTMES, APTMES subsequently links to BS3 which in turn binds fibrinogen.....	22

Figure 1-8 Tread milling process of actin, with addition and dissociation of actin monomers happening at opposite ends of the filament. Thymosin would act to sequester the actin monomers (shown in orange); permission to use the image acquired from the author (1). 26

Figure 2-1 Experimental set up for platelet aggregations under flow. The direction of blood flow is indicated by the arrows, and flows from the blood reservoir, to the flow cell chamber under the microscope, back to the pump and returning to the reservoir. 34

Figure 3-1 Variations in blocking agents do not affect fibrinogen dot peeling; the same extent of peeling is apparent for each type of blocking agent used, indicating the cause of peeling is not the process of blocking..... 38

Figure 3-2 Images of FITC-fibrinogen immobilized on the surface of PDMS using varying lengths of plasma oxidation and varying percent volumes of APTMES in ethanol. The best combination of time in plasma oxidation and percent volume of APTMES in ethanol was 60 second and 5% because it produced no peeling and a distinct edge. 40

Figure 3-3 A comparison of the adhesion curves for platelets in flow cell chamber experiments run over immobilized fibrinogen. Platelets labeled with Cell Tracker Green CMFDA dye show inhibited ability to bind fibrinogen. 42

Figure 3-4 A comparison of images taken of the PDMS surface over the time course of a flow cell chamber experiment. Platelets labeled with CMFDA dye show markedly reduced ability to adhere to immobilized fibrinogen, while platelets labeled with FITC do not (time measured in seconds). 43

Figure 3-5 Photobleaching of platelets labeled with FITC compared to platelets labeled with Bodipy-FL. Over the time-course of the flow cell chamber experiment, it is clear that Bodipy-FL labeled platelets are able to reflect the increase in platelet adhesion, while the steady decline in fluorescence seen in FITC labeled platelets indicates a photobleaching effect of platelets adhered to immobilized fibrinogen (photobleaching shown as a percent of the adhesion value at the time decay begins; n=4). 45

Figure 3-6 Platelets treated with excess protein of interest were subjected to a 5% isopropanol wash, and the wash was subjected to SDS-PAGE. The grey squares indicate where the law of mass action was successful in depositing excess amounts of protein onto the surface of the platelet. Using densitometry measurements in ImageJ the area under the curve was calculated to be (in order from left to right) 1276, 1156, 2191, 1229, 2741 and zero. 47

Figure 3-7 Verification of Mass Action deposition of redox modified or native state PDI onto the surface of isolated platelets. PDI is labeled with FITC (green) and EITC (red); the uniform colour verifies deposition onto the entire surface of the platelet. 49

Figure 3-8 Fluorescence scan of i) EITC and ii) FITC labeled PDI, verifying the presence and fluorescence of the bound fluorophore 50

Figure 3-9 Verification of redox state of PDI by the Di-Eosin-GSSG Assay (@540 nm). Reduced PDI cleaves Di-Eosin at the GSSG disulfide, causing an increase in fluorescence. Oxidized PDI does not cleave the disulfides, thereby not producing an appreciable increase in fluorescence. Arrow indicates point at which PDI was added. 52

Figure 3-10 Initial rates of aggregation of isolated platelets incubated with PDI in various redox states; activated with 1 unit/mL thrombin, there is no significant difference in initial rates of aggregation between any of the treatments (n=31)..... 53

Figure 3-11 Average kinetics of platelet adhesion to immobilized fibrinogen under flow. Isolated platelets were pre-treated with or without excess PDI (1 μ M). There is no significant difference between adhesion rates with or without excess PDI (n=3).... 55

Figure 3-12 Total theoretical aggregation curves depicting platelet adhesion to immobilized fibrinogen under flow. Theoretical curves are constructed based on the initial rates of adhesion for each trial (n=3)..... 56

Figure 3-13 Kinetics of platelet adhesion to immobilized fibrinogen under flow when treated with reduced or oxidized PDI, GSH or GSSG. It was determined that there is no statistical difference between any of the treatment states. 57

Figure 3-14 Concentration of free thiols in post flow plasma as a percent of the pre-experiment thiol concentration. The measured thiol concentration in plasma from the oxidized and reduced trials verifies that the redox state of the flow cell chamber environment remained oxidized and reduced respectively throughout the experiment..... 59

Figure 3-15 Initial rates of platelet aggregation following uncubation with 1 μ M b-b'. No statistical difference in the initial rates of aggregation was found between control and b-b' treated platelets (activated by thrombin (1 U/mL)) 61

Figure 3-16 Average kinetics of b-b' treated platelet adhesion to immobilized fibrinogen under flow. There is no statistical difference found between treated and untreated platelets (n=5). 63

Figure 3-17 SDS-PAGE and western blot analysis of isolated platelet ethanol wash, identifying Hsp70 on the surface of the isolated platelet.....	65
Figure 3-18 Kinetics of Hsp70 treated platelet adhesion to immobilized fibrinogen by activated platelets. No difference was found between Hsp70 treated and untreated platelets.	66
Figure 3-19 Images from a flow cell chamber experiment depicting the progression of adhesion of Bodipy-FL labeled platelets to immobilized fibrinogen, when pre-treated with Hsp70 or left in their native state.....	67
Figure 3-20 Initial rates of aggregation of platelets treated with varying doses of TB4 in the turbidity assay (* = significant difference when $P < 0.05$; $n=5$).....	69
Figure 3-21 Kinetics of platelet adhesion to immobilized fibrinogen under flow conditions at varying doses of TB4 ($n=3$).....	71
Figure 3-22 T β 4- fibrinogen binding curve. Fibrinogen was immobilized on PDMS in a 96-well plate while EITC labeled T β 4 was added at varying doses. The resultant binding curve displays a relationship akin to first order kinetics, excepting the decrease in binding that occurs above [TB4] of 30 $\mu\text{g/mL}$ ($n=4$).....	73
Figure 3-23 Initial rates of aggregation of platelets in a turbidity assay shown as a percent of control. Platelet aggregation was measured in the presence or absence of TB4 and fibrinogen. A peak at [TB4] 5 $\mu\text{g/mL}$ correlates with the strong binding seen in the TB4-fibrinogen binding curve; in the presence of fibrinogen this peak in aggregation disappears ($n=4$).....	74
Figure 4-1 Consensus sequences between fibrinogen and T β 4 that may produce a binding site for T β 4 on fibrinogen (images acquired from NCBI MMDB (83)).....	82

LIST OF ABBREVIATIONS

4E-BP1	Eukaryotic Initiation factor 4e binding protein 1
ADP	Adenosine diphosphate
APTMES	aminopropyltrimethoxysilane
Bodipy-FL	BODIPY® FL <i>N</i> -(2-aminoethyl)maleimide
BS ₃	Bis(Sulfosuccinimidyl) suberate
BSA	Bovine Serum Albumin
CMFDA	5-chloromethylfluorescein
DiE-GSSG	Di-Eosin GSSG
DMS	Demarcation membrane system
DSS	Disuccinimidyl suberate
DTNB	5,5'-Dithio-bis (2-nitrobenzoic acid)
DTT	dithioltrietol
eIF-4e	Eukaryotic initiation factor 4e
EITC	Eosin isothiocyanate
ER	Endoplasmic reitculum
FAD	Flavin adenine dinucleotide
GSH	Reduced Glutathione
GSSG	Oxidized Glutathione
Hsp70	Heat Shock Protein 70
IL-1β	Interleukin 1β
M ⁷ -GTP-cap	Methyl-7-guanosine triphosphate mRNA cap
NO	Nitric oxide
PAR-1	Protease activated receptor-1
PDI	Protein Disulfide Isomerase
PDMS	polydimethylsiloxane
PTFE	Polytetrafluoroethylene
RSNO	S-Nitrosylated compounds
SDL	Specificity determining loop
SDS-PAGE	SDS-polyacrylamide gel electrophoresis
TB	Terrific Broth
TXA ₂	Thromboxane A ₂
Tβ4	Thymosin beta 4
VWF	Von Willebrand Factor

Chapter 1 GENERAL INTRODUCTION

1.1 Platelets

1.1.1 Introduction

Platelets are small anucleate cellular structures that exist in the blood and are involved in the processes of hemostasis, wound healing and atherosclerosis. They are produced by mature megakaryocytes that are generated by the proliferation and differentiation of hematopoietic stem cells through megakaryocytic progenitors (3). Platelets carry out their primary function in hemostasis and wound repair, controlling bleeding upon vascular injury through a complex series of events. In short, platelets are able to sense the vessel wall injury, adhere to the site of injury, undergo morphological changes that attract other platelets to the site of the injury and begin formation of a tough plug that halts bleeding and begins the first stages of healing. Many bleeding disorders are caused by platelet dysfunction, such as Thrombocytopenia and VonWillebrands disease, and result in increased bleeding times or absence of clotting in patients. These disorders are very difficult to treat and if handled carelessly can result in injury and death.

1.1.2 Platelet Formation

Platelets are formed by Megakaryocytes, myeloid cells that reside in the bone marrow but can be found in the yolk sack and fetal liver prior to the time when marrow cavities have formed in the bone. Megakaryocytes develop from pluripotent human stem cells. The process of platelet formation, outlined in figure 1-1, begins with Megakaryocytes enlarging in a process known as endomitosis; which is promoted by the signaling

Chapter 1: General Introduction

molecule thrombopoietin. In endomitosis DNA is replicated up to 64 fold per cycle, and the nuclear envelope begins to break down. However, normal cell replication fails to proceed, and is halted at anaphase B, therefore bypassing telophase and cytokinesis. After the nuclear envelope reforms, there is a range of 4N up to 128 N per megakaryocyte (4). At the same time, the demarcation membrane system (DMS) matures, constituting a tubule network that associates with the plasma membrane and is thought to act as a reservoir for proplatelet production (5).

The open canalicular system, an open channel system designed for α -granule shuttling, is also formed during the cell expansion phase, prior to proplatelet production. The packaging of α -granules begins at this stage of cell expansion, with VonWillebrand Factor (VWF), receptors and other important platelet associated proteins shuttled into the secretory granules from the megakaryocyte. Other important platelet proteins such as fibrinogen are collected from the extracellular space via endocytosis/pinocytosis and also packaged into α -granules. Platelet biogenesis begins with the creation of proplatelets, or long pseudopodia-like extensions of the megakaryocyte cytoplasm driven by the thick linear bundles of microtubules in the proplatelet shaft. The polymerization and elongation of the microtubules appears to be dynein-facilitated, with the tubules growing both toward the body and towards the free end at which point the tubule rounds and re-enters the shaft, giving the bulbous appearance at the free end. One platelet will develop from each of these long proplatelet extensions; however, extensive end amplification allows bifurcation of proplatelet extensions; figure 1-1 depicts the process of platelet biogenesis and the extensive end amplification that can occur. Organelles and α -granules

Chapter 1: General Introduction

are shuttled to the proplatelet tip along the microtubules. Over time the pseudopodial extensions taper, and the platelet pinches off from the megakaryocyte (2).

Chapter 1: General Introduction

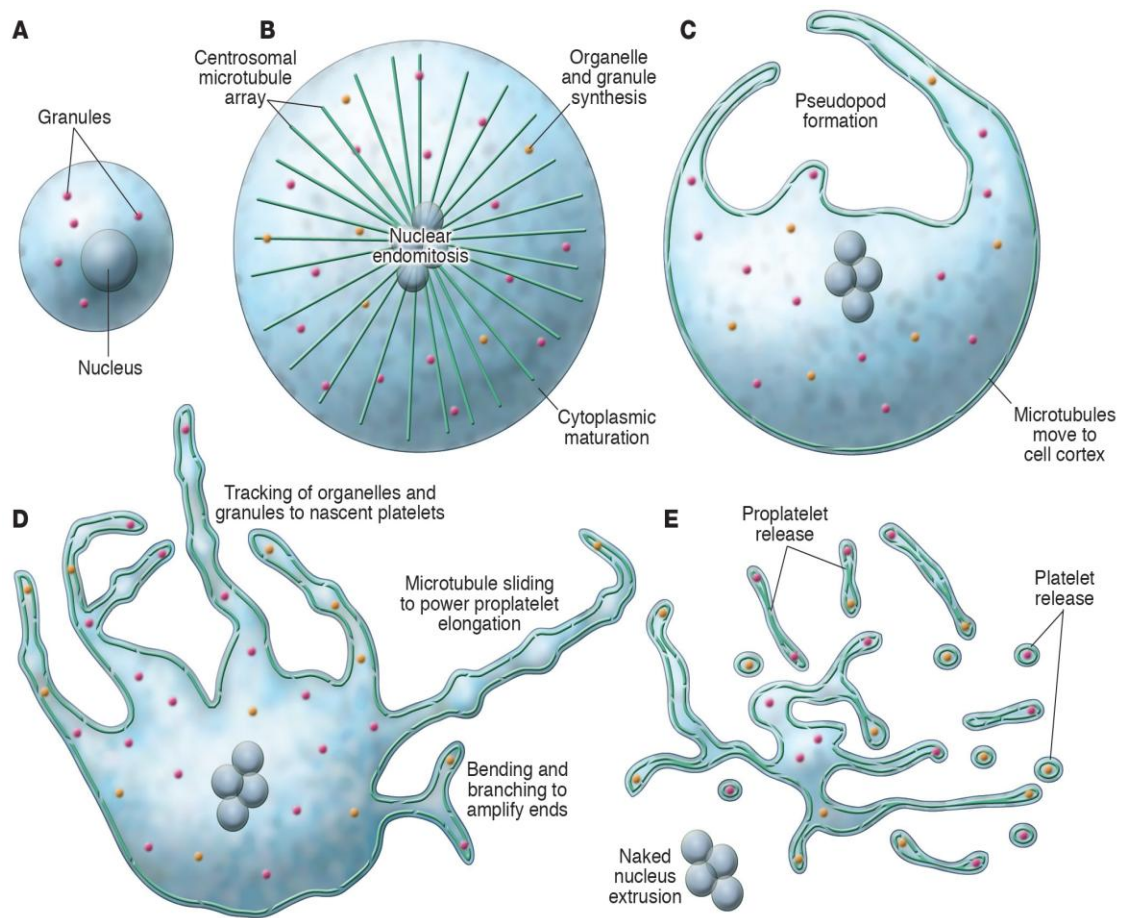


Figure 1-1 Megakaryocyte platelet biogenesis (2)

1.1.3 Platelet Activation

Platelets are activated by many different agonists, and are capable of responding to these agonists in a relatively redundant way. The list of physiologically relevant agonists includes thrombin, adenosine diphosphate (ADP), epinephrine, calcium ionophores (A 23187), fibrinogen, collagen and thromboxane A₂ (TXA₂) (6). Upon activation by an agonist, platelets undergo morphological changes mediated by cytoskeletal components, extending filopodia from the cell and releasing dense and α -granules into the extracellular space. Secreted compounds serve to further activate the platelet from which they were released, to attract and activate passing platelets, to initiate wound repair and to play a role in inflammation (7). As platelets become activated, they adhere to the site of vessel injury via cell surface integrins and receptors, become sticky and irregularly shaped and spread across the area of attachment. The contents of the secreted α -granules activate nearby platelets, causing them to become sticky and adhere to one another as well as those that have bound to the site of injury, forming a clot. The release of fibrinogen and thrombin allows the production of fibrin monomers, which cross-link to form a mesh that strengthens and reinforces the clot, preventing further blood loss. The multitude of signals capable of activating platelets establishes a failsafe mechanism, to ensure blood loss is minimal even if one or more signaling systems are impaired.

1.1.4 Thrombin Activation

Thrombin is a 36 kDa serine protease that is produced from a zymogen conversion of prothrombin in the coagulation cascade of activated platelets. Thrombin converts fibrinogen to fibrin monomers, as mentioned before, but also elicits shape change in

Chapter 1: General Introduction

platelets, release of platelet activators via α -granules and mobilization of P-selectin to the cell surface (8). Thrombin also exerts effects on other cells, including eliciting cytokine production in the endothelium and acting as chemo-attractive factors for monocytes and lymphocytes (8). Active thrombin exerts its effects upon cells by communicating with the human protease activated receptor-1 (PAR-1), cleaving it between Arg41 and Ser42 at the N-terminus thereby exposing a new amino terminus (9). This new N-terminus acts as a tethered ligand, activating itself and allowing coupling with G-protein coupled receptors (GPCR) such as $G_{12/13}$, G_q and G_i (8), activating a milieu of intracellular signaling cascades such as those shown in Figure 1-2.

1.1.5 Integrin Activation

Integrin molecules are adhesion receptors that reside in the plasma membrane of platelets and other cells, to function as cell adhesion molecules and receptors. They exist as glycosylated heterodimers composed of transmembrane α and β subunits that are non-covalently associated; each subunit possesses a large extracellular domain, a single transmembrane domain and a small cytoplasmic domain. (10)

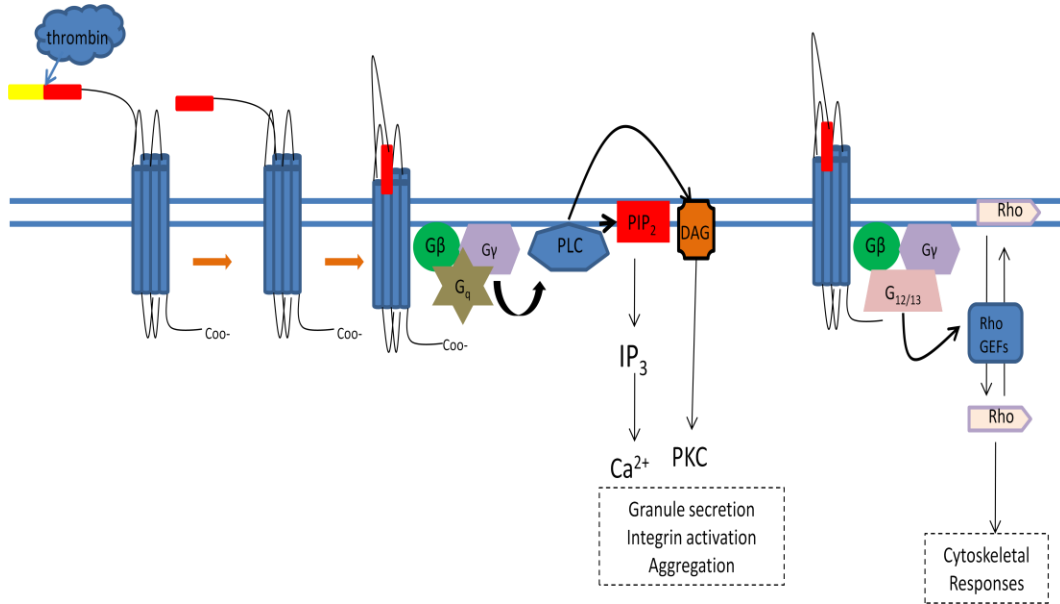


Figure 1-2: Downstream targets and effectors following proteolysis of PAR-1 by thrombin in platelet aggregation.

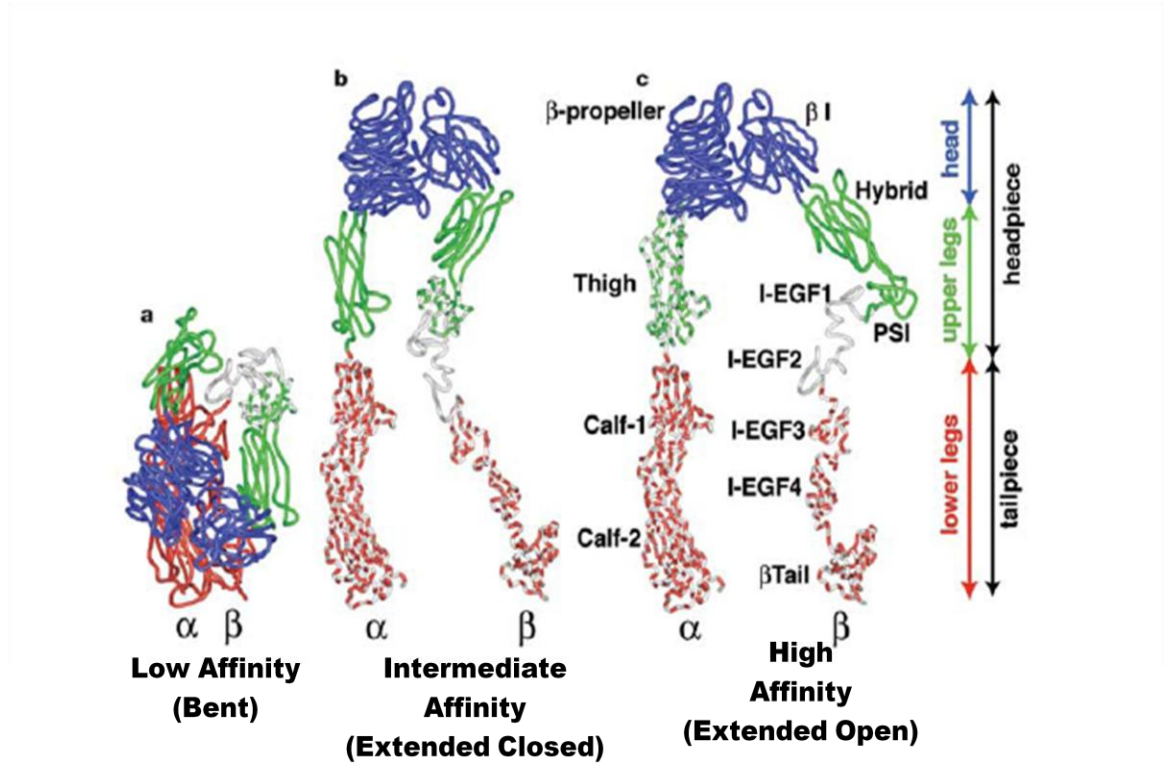


Figure 1-3. Integrin $\alpha_2\beta_3$ extracellular domain structure and affinity states

(10). When in the bent conformation the integrin assumes a low affinity state; as it moves from the extended closed conformation to the extended open conformation, the affinity increases achieving the extended open conformation once bound to fibrinogen. In inside-out signaling, interactions between the lower legs are disrupted, initiating the switchblade unfolding of the integrin.

Chapter 1: General Introduction

Integrins usually exist in a low-affinity binding state until activated via intracellular signals; this is termed ‘inside-out’ activation, a key step in integrin activation during platelet aggregation. As shown in figure 1-3, integrins assume many different conformations dependent upon the affinity state, moving through a bent conformation into an extended conformation with a closed headpiece, then to an extended conformation with an open head piece when going from lowest to highest affinity states respectively (11). The $\alpha_{2B} \beta_3$ integrin is platelet specific, and assumes the extended open conformation once bound to fibrinogen; the binding site for fibrinogen is a pocket loop that forms on the integrin head piece between the α_{2B} β -propeller and the β_3 -I domain specificity determining loop (SDL) (12). Inside-out signaling is initiated by activators (such as Talin-H) binding on the cytoplasmic face of the integrin, disrupting the hydrophobic and electrostatic interactions between the membrane proximal helices of the α_{2B} and β_3 cytoplasmic tails (13). Disruption of the binding between the membrane proximal helices triggers events that transmit the signal through the transmembrane segments to the extracellular domain. The exact mechanism of this signal transfer in the transmembrane domain is controversial; however it appears to cause disruption of the interactions in the extracellular domain between the lower α and β legs, further destabilizing the bent conformer’s headpiece-tailpiece interaction, resulting in a switchblade-like opening of the integrin into the extended conformation. Recent evidence also suggests that extracellular domain conformational changes resulting in a high affinity state are dependent upon disulfide bonding pattern changes between the many cysteine residues in the extracellular subunits (14-15). It has been shown that the exposure of free thiols is necessary for integrin binding, therefore thiol-dependent

ligation in $\alpha_{2B} \beta_3$ integrin may be required for integrin adhesion to fibrinogen (16). This points towards a possible role for protein disulfide isomerase (PDI) in platelet activation on the cell surface, though there remains controversy about whether integrins retain their own isomerase activity or whether an external isomerase is required.

1.1.6 Heat Shock Protein 70 on the Platelet Surface

Heat Shock Protein 70 (Hsp70) is a well known intracellular protein that is responsible for molecular chaperone function: a director of proper protein folding and unfolding, acting as a sensor for lethally mis-folded and aggregated proteins that can lead to cell death, or apoptosis. However there is recent evidence that Hsp70 is secreted from cells through three possible pathways and can have extracellular functions related to immunity and inflammation. These possible pathways include: secretion from an endolysosome; leakage from necrotic or apoptotic cells; or packaging and release in vesicles that bleb from the plasma membrane then lyse to release their contents (17-18).

After finding Hsp70 in supernatant of a platelet surface ethanol wash, a hypothesis that Hsp70 has a role in platelet aggregation on the external surface of the cell was developed (unpublished data). In the literature, Hsp70 has been investigated for its roles in the vasculature, with speculation that elevated levels of Hsp70 may protect against cardiovascular disease (19-20). As well, Hsp 70 levels in type I diabetic patients have been found to be inversely associated with macro and micro-vascular complications (21). In pediatric Immune Thrombocytopenic Purpura patients—an autoimmune disease that destroys platelets-- increased levels of plasma antibodies against Hsp70 have been discovered (22), and there has been some speculation that heat shock proteins alongside protein phosphatases have a role in platelet aggregation (23). All of this research points

to a role for Hsp70 in hemostasis and thrombosis, however, what that role is has yet to be determined.

1.2 Protein Disulfide Isomerase

1.2.1 Introduction

Protein disulfide Isomerase (PDI) is a ubiquitous 58 kDa thiol-disulfide oxidoreductase protein found in the endoplasmic reticulum (ER) of eukaryotic cells. It is a member of the thioredoxin superfamily of proteins, and is capable of disulfide exchange (24). In the ER, PDI is responsible for disulfide bond breakage, formation and rearrangement necessary for proper protein folding (25). Disulfide bonds are important for stability of protein structure and as redox responsive regulatory switches, all contributing to cell viability. Although PDI is largely considered to be an ER-localized protein due to its c-terminal KDEL retention signal (26) it has been found in other locales including the surface of human platelets (27), as a non-catalytic sub-unit of prolyl 4-hydroxylase (28) and as a subunit of the microsomal triglyceride transfer protein (29); however, PDI's full contribution in all of these respects has not yet been completely defined.

1.2.2 Domain Structure and Catalytic Activity

PDI is a five domain protein with overall domain structure of **a-b-b'-a'-c**. Each of the a, a' and b, b' domains all adopt the secondary structure of the thioredoxin fold, with the sequence $\beta\alpha\beta\alpha\beta\beta\alpha$ (30). The crystal structures of the **a** and **b** domains are shown

Chapter 1: General Introduction

in figure 1-4, with the thioredoxin fold shown in blue. Within the N-terminus of the second α -helix of the **a** and **a'** domains are the active site motif sequences— Cys-Gly-His-Cys—which are analogous to the thioredoxin motif sequence of –C-X-X-C – and constitute the independent active sites capable of thiol oxidation, reduction and Isomerization (31-32). The crystal structure of PDI has been researched most recently by Nguyen et al. in 2008 who have discovered that the molecule forms a ‘boat’ shaped arrangement, rather than the ‘twisted-U’ originally reported by Tian et al in 2006, such that the two **a** domains do not necessarily face each other across the catalytic cleft as was previously thought; the **b** and **b'** domains form a rigid platform from which the **a** and **a'** project, with the **a** domain being the more flexible of the two (33-34). As a result PDI appears to possess a more adaptive and flexible catalytic pocket than was originally thought, which is able to bind substrates of many different sizes and conformations (33, 35). The **b** and **b'** domains have been characterized as protein binding domains due to the hydrophobic residues within these domains lining the inside of the catalytic pocket, and are therefore thought to be responsible for proper protein positioning next to the catalytic domains as they are themselves catalytically inactive (36). The catalytic activity of PDI as shown in Figure 1-4, is capable of forming, breaking or isomerizing mis-paired disulfide bonds using redox reaction chemistry: one chemical species attains a higher oxidation state through the gain of electrons, while the other species is reduced and loses electrons.

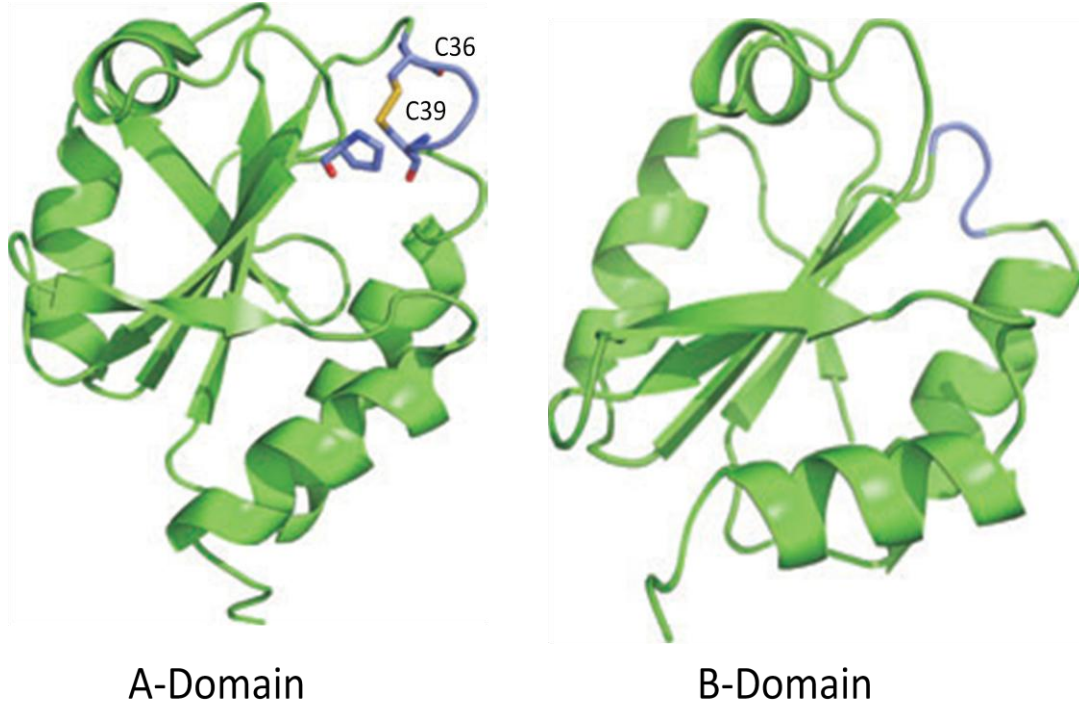


Figure 1-4 The a and b domains of human PDI. The a domain contains five-stranded mixed b-sheets surrounded by four a-helices. The active site motif lies between C36 and C39 at the N-terminus of a2. There is virtually no sequence similarity between the domains (32)

Chapter 1: General Introduction

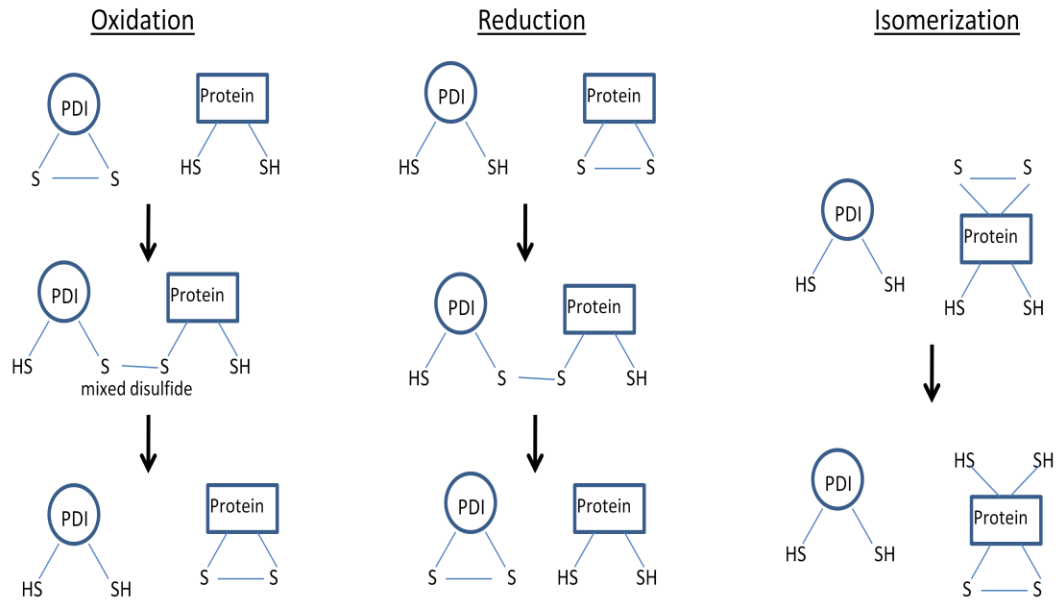


Figure 1-5 The redox-dependent activities of PDI. By forming mixed disulfides with cysteine residues, PDI is able to form and break disulfide bonds producing a protein with free thiols, disulfide bonds or shuffled disulfide bonds

Chapter 1: General Introduction

Free thiol groups on unpaired cysteines can be oxidized by PDI to form a disulfide bond between two sulfur atoms, both of which attain a -1 oxidation state as the protons are transferred to the PDI active site thereby reducing it to a dithiol state (37). An interesting and recently discovered property of PDI is that it can exist as a dimer in solution and in the ER, with 9.7% of the monomer surface being buried; of this buried portion, 17% of the contact interface is contributed by the **a** domain, with the remaining domains contributing the balance equally (34). This further suggests the increased flexibility of the **a** domain, possibly making it the primary mediator of the enzyme's interaction with proteins of many differing sizes and conformations.

The **b** domain appears to possess molecular chaperone properties as it is able to bind small peptides, allowing PDI to recognize and interact with proteins and cooperating with the **a** and **a'** domains for larger protein interactions. These molecular chaperone domains allow for positioning of substrates in the active site in such a way to expose buried thiols or disulfide bonds, to prevent improper interactions between partially folded intermediates, for targeting the thiols or disulfide bonds that specifically need attention and for recognition of improperly folded proteins in more than one intermediate state (32). The binding of proteins to PDI at one site appears to happen with fairly low affinity; however, the binding is multiplicative with each additional binding site contributing to an increase in binding affinity. It is thought that as the proper protein folding and structure is established by forming proper native bonds, the protein will bind to fewer and fewer sites on PDI, eventually having the lowest binding affinity when proper native conformation is achieved. The acidic C-domain possesses the KDEL-ER

retention sequence, and does not appear to contribute to the enzymatic function of the protein (38).

The redox state of PDI's active site is largely dependent on the ratio of reduced to oxidized glutathione ([GSH]/[GSSG]) in the compartment in which it resides (39); in the ER this ratio is approximately 3:1, creating a reducing environment. The oxidation of PDI in the ER is thought to be due in large part to Ero1, an oxidative exchanger which recharges PDI by reducing flavin adenine dinucleotide (FAD) to FADH₂, using molecular oxygen as a terminal electron acceptor, thereby producing H₂O as a by-product (40). *In vitro*, PDI's active site thiols can also be reduced or oxidized by GSH or GSSG, dithioltrietol (DTT) and reactive oxygen species (41).

1.2.3 PDI in Platelet Aggregation

Potential targets for PDI on the platelet cell surface include the collagen receptor and surface integrin $\alpha_2\beta_1$ (16), and the fibrinogen receptor and integrin $\alpha_{2b}\beta_3$ (15). These all appear to require disulfide bond exchange or re-arrangement to induce an active state conformation which initializes signalling pathways that subsequently activate platelet aggregation (42). A proposed disulfide bond re-shuffling mechanism shown in Figure 1-6 outlines how PDI might interact with the extracellular integrin disulfide bonds to initiate an active state conformation. The $\alpha_2\beta_1$ collagen receptor has been shown to form intra-receptor stabilizing disulfide bridges during its high affinity state (43), which suggests a role for a disulfide isomerase in switching the integrin to its active conformation. This was corroborated by evidence that platelet adhesion to collagen was inhibited by the anti-PDI antibody RL-90 (16).

Chapter 1: General Introduction

Yan et al have shown that in the $\alpha_{2b}\beta_3$ integrin, multiple unpaired cysteine residues exist in the β_3 subunit which are postulated to comprise a key modulatory redox site for integrin activation. The importance of the cysteine-rich domain in the integrin β_3 subunit and the possible role for PDI regulatory activity at this site are supported by the following discoveries. The conformational changes that coincide with integrin activation have been mapped to the disulfide rich region of the β_3 subunit (44). Cysteine substitutions in the EGF-like domains of the β_3 subunit were found to cause decreased surface expression of the integrin when double or single mutations in the EGF-like 3rd and 4th domains were applied; additionally several different cysteine mutations in the EGF-3-like domain caused constitutive activity of the receptor, while disruption of the cys567-cys581 disulfide bond in the EGF-4-like domain caused a completely inactive state (45). DTT has been shown to initiate a slow acting platelet aggregation through reduction of disulfide bonds (46). Finally PDI inhibitors have been shown to attenuate $\alpha_{2b}\beta_3$ activation on the surface of the platelet (47).

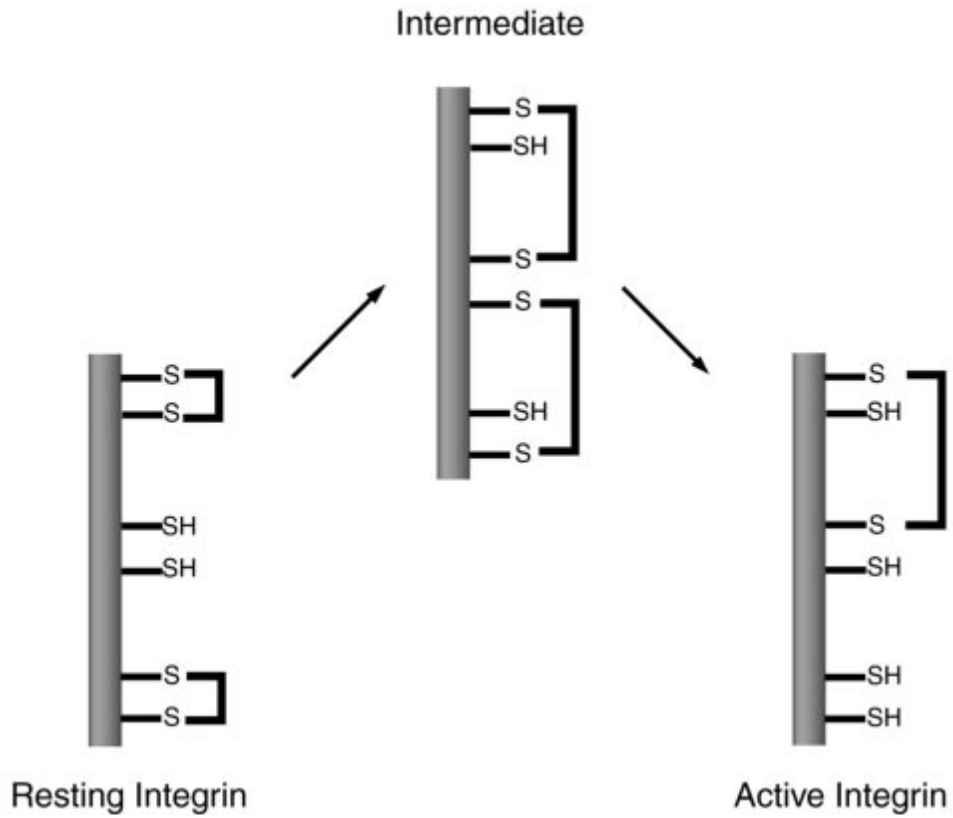


Figure 1-6 A model of the proposed disulfide bond shuffle that occurs in integrins on the platelet surface. Resting and active integrins differ in the number and positioning of unpaired cysteines (44).

1.2.4 PDI in Other Roles

Although PDI clearly has many roles as an independent protein, it can also function as a subunit of other larger enzymes. The enzyme human prolyl 4-hydroxylase acts upon collagen and other proteins forming 4-hydroxyprolines by hydroxylating proline residues, which are necessary for stabilizing the collagen triple helix (28). The enzyme is an $\alpha_2\beta_2$ tetramer, where PDI serves as the β -subunit and one of its roles is to retain prolyl 4-hydroxylase in the ER via the C-terminal KDEL retention signal. PDI also acts as a chaperone for prolyl 4-hydroxylase by keeping the α -subunits in a nonaggregated and catalytically active form; this activity is unable to be mimicked by any substitute non-PDI chaperone proteins such as Hsp70 (48). The same molecular chaperone activity that PDI contributes to prolyl 4-hydroxylase appears to also occur when it is a subunit of the enzyme microsomal triglyceride transfer protein. The microsomal triglyceride transfer protein is a soluble ER $\alpha\beta$ dimer protein that is required for the assembly and secretion of very-low-density lipoprotein from hepatic cells and chylomicrons from enterocytes. PDI is the β -subunit in this protein as well, where again its role appears to include ER retention of the $\alpha\beta$ dimer and maintaining the solubility and catalytic activity of the α -subunits, but not appearing to contribute to the enzymatic activity of the dimer with its usual isomerase activity (49).

PDI is also capable of denitrosating S-nitrosoglutathione and other S-nitrosylated compounds (RSNO) resulting in the release of nitric oxide (NO), as reported by Sliskovik et al in 2005. NO is a ubiquitous signalling molecule which is especially significant in the cardiovascular system, where release of NO into the vasculature induces vasorelaxation and inhibits platelet function. It has been suggested that there exists a role for PDI in catalyzing transmembrane transfer of NO, first relieving it from an RSNO

source (50). Studies on the mechanism of PDI denitrosation of S-nitrosothiols suggests that the cysteines in the CXXC motif of the active sites attack the RSNO substrate, undergoing a transnitrosation reaction and forming a nitrosyl disulfide intermediate, which ultimately results in release of NO leaving the PDI active site oxidized. Furthermore when NO levels are high, PDI is capable of accumulating NO within its hydrophobic domains, storing it as N_2O_3 (a potent nitrosating agent), thus nitrosating the nearest vicinal thiols within PDI and forming PDI-SNO. In this manner PDI can act as a sink for NO, carrying it across the membrane where cell surface PDI denitrosates it, releasing it into the extracellular environment.

1.3 Flow Cell Methodology Development

1.3.1 Introduction

As previously noted, the role of platelets in hemostasis and thrombosis begins with adhesion to the site of vascular injury. The current methods for assessment and investigation into platelet adhesion to various matrices under various conditions are not sufficiently reliable, are expensive and are often not physiologically relevant. Popular methods include passing of blood over coverslips coated with proteins such as fibrinogen (51), aggregometry in spectrophotometers and plate readers; the bleeding time test; impedance aggregometry in whole blood (52); Platelet Function Analyzers which measure occlusions of apparatus as an indication of wound closing time (53); flow cytometry as a measure of platelet activation and sensitivity to agonists using fluorescently conjugated monoclonal antibodies (54); and measurement of secreted α -granules and their contents in response to agonists. Our group has sought to create a

Chapter 1: General Introduction

reliable, inexpensive and accessible method for investigating platelet adhesion and aggregation in a physiologically relevant setting using teflon boundary flow chambers, constructed internally with a polydimethylsiloxane (PDMS) surface coated with proteins of interest.

1.3.2 Surface Chemistry

The PDMS surface was manipulated chemically to ensure that any proteins applied there would be tethered to the surface, rather than merely associated with it. The otherwise inert PDMS, when subjected to plasma oxidation, possesses exposed hydroxyl groups on the surface. These hydroxyl groups provide the ideal place for linker compounds, such as the one used in this study 5% aminopropyltrimethoxysilane (APTMS), to react. The exposed amines of APTMS furthermore provide an excellent target for subsequent linker compounds such as the one used in this study, the amine reactive bis(sulfosuccinimidyl) suberate (BS₃), and other linkers such as disuccinyl suberate (DSS). The final compound BS₃ provides the last link between the aforementioned covalent linkers and the protein of interest, which in this study was fibrinogen, but could be a variety of proteins including collagen. The final chemical scheme of the immobilization of fibrinogen onto plasma oxidized PDMS is shown in Figure 1-7.

This method allows investigators to pass whole blood over the PDMS surface under a microscope, and quantify platelet adhesion to the proteins of interest, with the ability to add and manipulate many variables including, but not exclusively, compounds, shear stress rates, temperature and light.

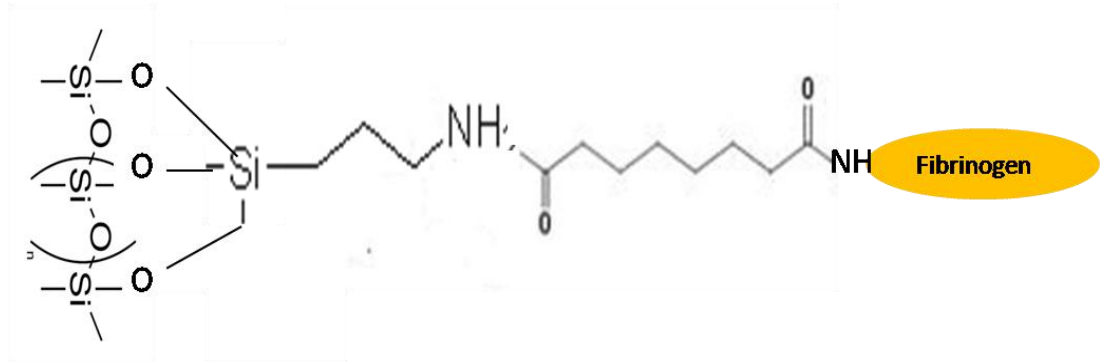


Figure 1-7 The surface chemistry of PDMS flow cells for immobilization of proteins. Plasma oxidation exposes hydroxyl groups on the PDMS surface that are bound by APTMES, APTMES subsequently links to BS3 which in turn binds fibrinogen.

1.4 Thymosin Beta Four

1.4.1 Introduction

The β -thymosins are small, acidic 5 kDa peptides that are ubiquitous and highly conserved among species. They were originally thought to be thymic hormones, but have since been identified as G-actin sequestering peptides participating in cell movement and cytokinesis (55-56). Thymosin β 4 (T β 4) is present in concentrations from 0.1 μ M up to 560 nM in a variety of tissues and cell types, including platelets, where its main role is to bind free actin, or G-actin, thereby inhibiting association with the F-actin filament (57-58). Specifically in platelets T β 4 has been shown in high concentrations, with levels of free T β 4 increasing after activation with thrombin corresponding to the polymerization of F-actin and a decrease in the levels of the T β 4-actin complex, allowing platelets to change shape and to elicit their physiological response in blood clot formation (59). T β 4 is also co-released with factor XIIIa (plasma transglutaminase) from platelets following activation with thrombin and is integrated locally into fibrinogen monomers and fibrin polymers within the hemostatic plug at their α C-domains (60-61). Decreased levels of T β 4 in cancer cell lines has been noted by various groups, and has led to postulated roles for T β 4 in the cell cycle and immunity (62). Sosne *et al* studied the effect of T β 4 administration on corneal epithelial wounds and found that T β 4 is also involved in wound healing and cell migration, as well as possessing anti-inflammatory and anti-apoptotic properties (63).

1.4.2 Domain Structure and Activity

Chapter 1: General Introduction

Thymosin β 4 is a peptide that is largely unstructured in water, but has a tendency to form α -helical structures in aqueous solutions containing fluorinated alcohols (64). Circular dichroism analysis has suggested that isolated T β 4 has an average of six helical residues and its actin-bound form contains up to 12 helical residues (65). Thymosin β 4 binds to actin with an equilibrium dissociation constant of $K_T = 1$ to $2 \mu\text{M}$ (66). Various molecules such as profilin and DNase 1 have shown competition with T β 4 for binding free actin, some due to steric overlap, with DNase 1 able to form a ternary complex with T β 4-actin (67). Recently Yarmola *et al* have shed greater light on this competitive binding scheme and determined that at concentrations higher than 5 - $10 \mu\text{M}$ the prevailing event is non-competitive inhibition, due to the existence of ternary complexes and allosteric changes in actin; however there have also been reports that intra-platelet concentrations of T β 4 range from 200 - $500 \mu\text{M}$ (57). In order to bind G-actin, the N-terminus of T β 4 must adopt an α -helical conformation, exposing an important hydrophobic residue ^6Met . When ^6Met is exposed the N-terminal binding motif $^{17}\text{LKKTETQ}^{23}$, and possibly also 6 important N-terminal amino acids, become properly positioned to participate either directly or indirectly in binding the C or N-terminus of actin between sub-domains 3 and 1 (67-69). Figure 1-8 depicts the actin filament formation process within the cell, tread milling between monomer addition on the barbed end by profilin and monomer disassembly on the pointed end by T β 4. The balance of these processes depends on concentrations of the regulators. However, T β 4 has two orders of magnitude higher affinity for ATP-G-actin (free) than ADP-actin which is contained within the polymer. Hence, the concentration of free actin in the cytoplasm is the main regulator of disassembly, and the concentration of free actin is heavily

Chapter 1: General Introduction

dependent upon the concentration of T β 4: once actin is sequestered by T β 4, the T β 4-actin complex no longer contributes to the free actin pool. The equilibrium is balanced as follows, where [TA]_{ss} is the T β 4-actin complex, [A]_{ss} is free G-actin, [T] is the concentration of T β 4 and K_T is the equilibrium constant (66):

$$[TA]_{ss} = [T]_0 \cdot [A]_{ss} / ([A]_{ss} + K_T)$$

The role of T β 4 appears to be vastly different on the surface of the platelet. There has been much research about the effects of T β 4 on endothelial cell migration as a chemoattractive factor in wound healing; also elevated levels of T β 4 have been discovered around areas of blood vessel and neuronal growth (70-71). As a result of these accumulated findings, there has been speculation that upon injury T β 4 is released from activated platelets and inserted into the fibrin/fibrinogen matrix that forms around the wound in an effort to keep the local concentration of T β 4 relatively high. A higher local concentration of T β 4 may be needed to stimulate the epithelial cell migration and angiogenesis necessary to close and heal the wound. The presence of T β 4 has also been associated with anti-inflammatory properties, and as such does not appear to stimulate macrophage migration (58). Although these effects of T β 4 have been researched and documented, the processes by which it contributes to wound healing, angiogenesis and platelet aggregation are not fully elucidated.

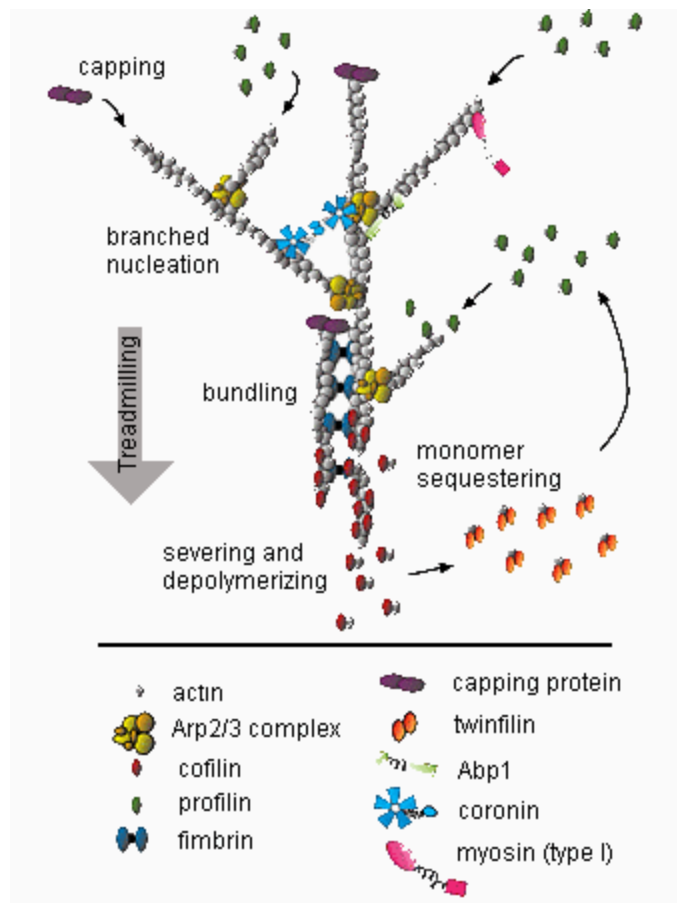


Figure 1-8 Tread milling process of actin, with addition and dissociation of actin monomers happening at opposite ends of the filament. Thymosin would act to sequester the actin monomers (shown in orange); permission to use the image acquired from the author (1).

OBJECTIVES

1. Optimize the flow cell chamber experiment: determine the cause of fibrinogen dot peeling and identify the most robust and effective platelet fluorescent label
2. Investigate the effects of excess platelet surface protein on platelet aggregation—
Protein disulfide isomerase for its potential role as a cell surface oxidoreductase, the b-b' subunit of protein disulfide isomerase for its potential role as a chaperone for the critical disulfides in the $\alpha_2\beta_3$ integrin, and heat shock protein 70 for its potential role as a platelet surface chaperone protein or ATPase.
3. Investigation into the effect of the redox state of platelet surface protein disulfide isomerase and the whole blood environment on platelet aggregation
4. Investigate the effects of Thymosin β_4 on platelet aggregation

Chapter 2 MATERIALS AND METHODS

2.1 Materials

Hepes (EMD); sodium chloride (ACD Chemicals Inc); Sodium phosphate dibasic (ACD Chemicals Inc); Potassium chloride (ACD Chemicals Inc); D-glucose (sigma); Trisodium citrate dehydrate (EMD); citric acid monohydrate (BDH Chemicals); 8 mL ACD Vacutainer Whole Blood Collection Tubes (VWR); fluorescein isothiocyanate (Fluka); dimethyl sulfoxide (EMD); Kanamycin (Sigma); Tryptone (Sigma); Yeast Extract (EMD Chemicals Inc); Potassium phosphate monobasic (ACD Chemicals Inc); Tris-HCl (ACD Chemicals Inc); Imidazole (Sigma); Lysozyme (Sigma); DNase 1 (Sigma); Phenylmethanesulfonyl fluoride (Sigma); Triton x100 (Sigma); 30% Acrylamide (Bio-Rad); Tris-(Hydroxymethyl) Aminomethane (ACP Chemicals Inc.); Sodium dodecyl sulfate (Sigma); Ammonium persulfate (Sigma); Temed (EMD Chemicals Inc.); Glycine (EMD Chemicals Inc); Methanol (U.W CCC); Glutathione sepharose 4B beads (GE Healthcare); Precision Protease (GE Healthcare); HIS-Select Nickel Affinity Gel (Sigma); Glutathione, oxidized (Sigma); Glutathione, reduced (sigma); Eosin Isothiocyanate (Fluka); EDTA (Fischer Scientific); G25 Sepharose (Sigma); Potassium phosphate (ACP Chemicals Inc.); Sylgard 184 Silicone Elastomer Kit (A.E Blake Sales Ltd.); 3-Aminopropyl-trimethoxysilane (Aldrich); BS₃ (Thermo Scientific); Fibrinogen (Sigma); CaCl₂ (ACD Chemicals Inc); Plasma Cleaner (Harrick Plasma PDC-32G); pump (Reglo Digital MS 4/6, model ISM 833, Ismatec); PTFE Teflon sterile tubing (0.031" X 0.062"); Microscope (Zeiss); Retiga EX, cooled Mono 12 bit Camera (Q Imaging); Northern Eclipse Software (Empix Imaging Inc); Cuvette (Sarstedt); Spectrophotometer (Agilent); Thrombin (Sigma); BODIPY® FL N-(2-

Chapter 2: Materials and Methods

aminoethyl)maleimide (Invitrogen); 5,5'-Dithiobis(2-nitrobenzoic acid) (Sigma); sodium acetate (Sigma)

2.2 Methods

2.2.1 Blood Acquisition

Blood was obtained from the arm veins of healthy volunteers and collected in blood collection tubes containing ACD. The tubes were stored upright at room temperature until the contents were used.

2.2.2 Platelet Isolation and Preparation

Whole blood was centrifuged at 400 RPM for 30 min at room temperature and platelet rich plasma (PRP) supernatant was decanted. 0.5 μ M Prostaglandin E₁ was added to PRP prior to centrifugation at 600 RPM for 15 min (72). Plasma supernatant was removed and stored at room temperature for later use in flow chamber experiments. The platelet pellet was carefully removed from the surface blood pellet, re-suspended in Hepes-ACD buffer and subsequently centrifuged at 600 RPM and re-suspended until the blood pellet was removed. Isolated platelets were stored resuspended in Hepes-ACD at room temperature on a nutator and used the same day. If the platelets were to be used in a flow chamber experiment they were labeled with fluorescein isothiocyanate (FITC) at a

Chapter 2: Materials and Methods

concentration of 48 $\mu\text{g/ml}$ for 10 minutes at room temperature, washed twice with re-suspension in HEPES-ACD and used immediately(73). The same procedure was used for platelets labeled with Bodipy®FL *N*-(2-aminoethyl)maleimide (Bodipy-FL) at a final concentration of 0.5 μM (74) and Cell Tracker Green 5-chloromethylfluorescein (CMFDA) at a final concentration of 2.5 μM (75).

2.2.3 Cloning of Hsp70

Cloning was performed by Tanya Marar under the supervision of Dr. Bulent Mutus and Dr. Sirinart Ananvoranich. The human hsp70 gene was cloned from the pEGFP hsp70 plasmid into the pET21a+ vector using EcoRI and HindIII restriction enzymes. A 1932 bp insert was generated with a C-terminal His₆tag. The vector was transformed into BL21 (DE3) pLysS *E. coli*.

2.2.4 Protein Purification

PDI, Hsp70 and the B-B' domain of PDI were all purified from BL21 (DE3) *E. coli*. Glycerol stocks were thawed at room temperature and used to inoculate 50 ml of autoclaved terrific broth (TB) containing kanamycin at a concentration of 25 $\mu\text{g/mL}$. After growing overnight, 1 ml of the culture was used to inoculate an identical 1 L of TB. Following 3 hours of growth the OD₅₄₀ was assessed and the culture was allowed to grow until it reached an OD of 0.4 to 0.6 was reached. The culture was then induced with 1 mM isopropyl β -D-1-thiogalactopyranoside (IPTG) and centrifuged at 6000 RPM for 30 min at 4° C. Cells were re-suspended in lysis buffer and incubated on ice for 20 min

Chapter 2: Materials and Methods

followed by sonication. The lysate was centrifuged at 12,000 RPM for 30 min at 4°C. The supernatant was run over a nickel affinity column in the case of both PDI and Hsp70 due to their His₆ tags, to isolate the protein of interest. The B-B' protein was isolated by running the lysate over Glutathione Sepharose 4B beads pre-washed in water and equilibrated in PBS+DTT. Precision Protease was added and incubated overnight with gentle agitation. The eluate in all cases was collected in several fractions and analyzed by SDS-PAGE, Western blotting (except TB4) and Bradford Assay.

2.2.5 Protein Disulfide Isomerase Preparation: oxidation, reduction and isomerization

To induce oxidation purified PDI was incubated overnight with oxidized glutathione (GSSG) at a final concentration of 0.01 M. The same was done to induce the reduced state of PDI, using reduced glutathione (GSH) at the same concentration. To produce PDI in the isomerization form a ratio of 4:1 GSSG:GSH was used with a total final concentration of 0.01 M. In all cases the PDI was incubated overnight at 4°C and then run over a G25 column to remove GSH/GSSG. PDI activity was assessed using the Di-Eosin-GSSG assay (DiE-GSSG) (39) and the level of activity was used as an indication of the level of oxidation of the PDI active site. For verification of deposition on the platelet surface, redox induced PDI was labeled with eosin 5-isothiocyanate (EITC) and fluorescein isothiocyanate (FITC) by incubation of PDI at minimum concentration of 2 mg/mL with 1 mg/mL EITC or FITC. Carbonate buffer at a concentration of 0.5 M and pH 8.0 was used as the main solvent, and DMSO was used to initially dissolve the EITC and FITC. After incubation overnight at 4°C, PDI was run over G-25 sephadex column and fractions were collected and subjected to Bradford Assay and fluorescence scans to

Chapter 2: Materials and Methods

verify protein concentration and fluorophore viability. Redox induced PDI was incubated with isolated platelets overnight at room temperature under gentle agitation. The platelets were washed twice with HEPES-ACD before being used for experimental purposes.

2.2.6 Spectrophotometer Turbidity Assay Experimental Procedure

Isolated unlabeled platelets, either treated or untreated, were added to HEPES-ACD in an acrylic 500 μL cuvette at a final concentration of 2×10^7 cells/mL. The cuvette was placed inside the Spectrophotometer, and absorbance was read in kinetics mode every 2 seconds at a wavelength of 595 nm. After the first 30 seconds, the activator Thrombin was added (final concentration 1 unit/ml) with a curved glass instrument termed a 'plumper' to enable quick, efficient addition combined with mixing. The total final volume of HEPES-ACD + platelets + thrombin was 500 μL . Two control treatments were utilized: one wherein HEPES-ACD was added in the place of thrombin and one wherein untreated platelets were used and activated by thrombin. The aggregation was allowed to run to completion.

2.2.7 Flow Chamber Assembly

Sylgard 184 Silicone elastomer base was combined with silicone elastomer curing agent in a 10:1 ratio respectively, to create PDMS. A glass cover slip formed the bottom of the chamber and was adhered to the square acrylic mold of the chamber with PDMS. After polymerization at 70°C for at least 25 minutes, the inside of the chamber was filled with more PDMS, using an acrylic and polytetrafluoroethylene (PTFE) tubing insert to

Chapter 2: Materials and Methods

create a negative entrance space for blood to pass into and out of the chamber. This was also allowed to cure at 70°C for at least one hour. The acrylic insert was removed revealing the negative space, and the final coating of PDMS was applied to the remaining area of coverslip that was exposed, to create an entirely PDMS-lined chamber. The flow cells were then subjected to plasma oxidation cleaning which allowed the normally inert silicone surface to contain exposed hydroxyl groups. A solution of 5% APTMES in ethanol was applied in a small (<1µL) dot to the surface of the PDMS and allowed to bind for 15 minutes. Following binding, BS₃ (final concentration 0.125 mM) was added on top of the APTMES dot followed immediately by type 1 fibrinogen in 0.88% saline (final concentration 0.005 mM) on top of the BS₃. The chambers were incubated at room temperature for at least 10 minutes before being used in the flow experiments.

2.2.8 Flow Chamber Experimental Procedure

Prior to use, the flow chambers were blocked with a 1 M pH 8 Tris solution for approximately 2 minutes. The flow cells were attached to an Ismatech pump as shown in the experimental set up in Figure 2-1. Red Blood Cells (RBCs) and plasma were recombined in a 1:1 ratio, and isolated, labeled platelets were added at a final concentration of 2.5×10^7 platelets/mL. The pump was run at a speed of 2.00 mL/min, and the entire experiment was run for 390 seconds. Images were taken every 10 seconds throughout the run with a Zeiss Microscope and Retiga EX, cooled Mono 12 bit camera using Northern Eclipse software. After the 8th image was taken, the platelet activator CaCl₂ was added at a final concentration of 4.6 mM.

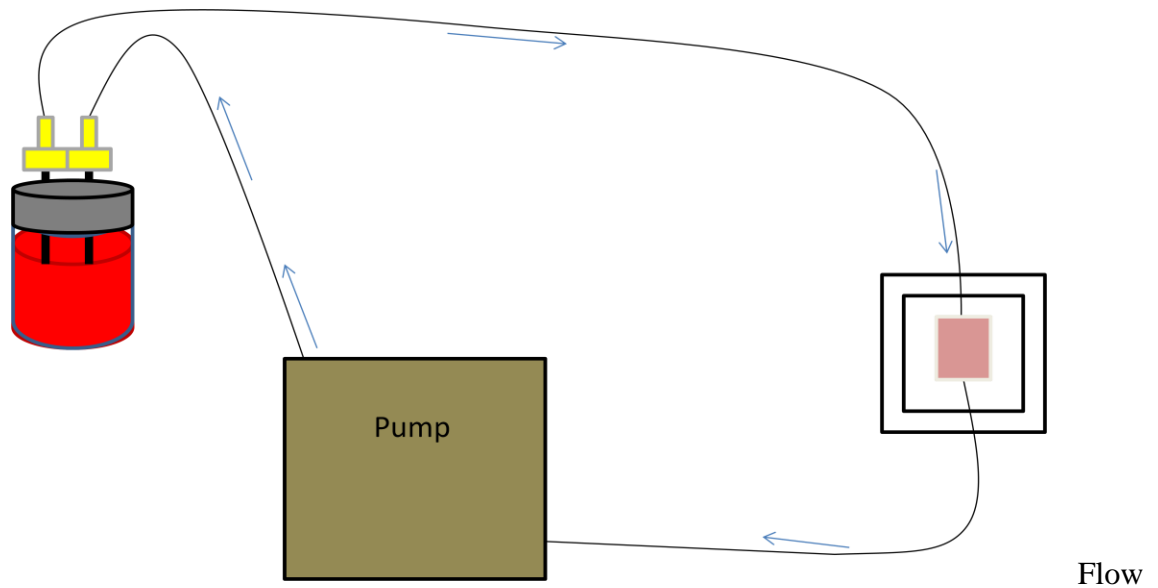


Figure 2-1 Experimental set up for platelet aggregations under flow. The direction of blood flow is indicated by the arrows, and flows from the blood reservoir, to the flow cell chamber under the microscope, back to the pump and returning to the reservoir.

2.2.9 Thymosin β_4 Fibrinogen Binding Assay

All necessary wells of a 96-well plate were filled with 50 μL of PDMS at a ratio of 10:1, base:curing agent. The plate was treated exactly as a flow cell, first exposing it to plasma oxidation then applying all necessary chemicals with an identical time course: 2 μL of 5% APTMES in ethanol followed by 2 μL of both 2 mg/mL BS_3 and 2mg/mL type 1 fibrinogen in 0.88% saline. $\text{T}\beta_4$ was labeled with eosin-isothiocyanate (EITC) at a concentration of 10 mM in the presence of 1 M bicarbonate solution pH 8.0, at room temperature in the dark for 2 hours under gentle agitation. The labeled $\text{T}\beta_4$ was run over G25 column in the dark to remove unbound EITC, and subjected to Bradford Assay to determine protein concentration. Before application of the labeled $\text{T}\beta_4$, the wells were blocked with 1 M Tris-base; after 2 min the Tris was aspirated from the wells, and the various concentrations of $\text{T}\beta_4$ were added to the wells: 0.01 $\mu\text{g}/\text{mL}$, 0.1 $\mu\text{g}/\text{mL}$, 0.5 $\mu\text{g}/\text{mL}$, 1.0 $\mu\text{g}/\text{mL}$, 5.0 $\mu\text{g}/\text{mL}$, 10.0 $\mu\text{g}/\text{mL}$, 30.0 $\mu\text{g}/\text{mL}$, 50.0 $\mu\text{g}/\text{mL}$, 100.0 $\mu\text{g}/\text{mL}$. The plate was incubated under gentle agitation for 2 hours in the dark before the wells were washed 3 times with PBS (pH 7.0) in the dark. The plate was read in a PerkinElmer Victor Multilabel Plate Reader using Workout 2.0 software.

2.2.10 5,5'-Dithiobis(2-nitrobenzoic acid) Assay

Plasma was isolated from whole blood by centrifugation at 400 RPM both before and after the flow cell chamber experiment. A 5,5'-Dithiobis(2-nitrobenzoic acid) (DTNB) solution was made using 50 mM sodium acetate (NaAc), 2 mM DTNB in water. A DTNB working reagent was made using 50 μL of the DTNB solution, 100 μL 1 M Tris solution pH 8.0, and water 840 μL . The DTNB working reagent was combined with the

Chapter 2: Materials and Methods

sample at a ratio of 10:1 DTNB to plasma sample. The solution was mixed well, then absorbance was read in the spectrophotometer at 412 nm.

2.2.11 Data Analysis

Spectrophotometric data was analyzed by determining the initial rate of aggregation as the slope of the line of the initial aggregation curve, between more than 4 points. Data from aggregations under flow were analyzed using the Northern Eclipse software. A rectangular trace with area 12,375 pixels was used consistently for all movies taken. The number of platelets bound and total fluorescence of the area within the rectangle were counted. All data were pooled and the Y for each image (where Y=fluorescence value) was subtracted from the Y_{final} to calculate the difference in total fluorescence across all images per movie. The natural Ln of the difference produced a plot with the slope equaling the rate constant. The rate constant was used to produce a theoretical curve using the equation:

$$Y = Y_{\text{final}} \times (1 - e^{(-1 \times \text{rate constant} \times \text{time})})$$

The rate constant of the theoretical curves was adjusted until the theoretical curve fit the actual curve +/- 0.002. This was done for each movie individually. Statistical significance was determined using the T-test with $p < 0.05$.

Chapter 3 RESULTS

3.1 Flow Cell Methodology

3.1.1 Optimizing the Surface Chemistry

Initially when beginning the use of the flow cell chambers, a previous protocol was used that included the use of 100% APTMES on the activated PDMS surface. Upon closer examination of the immobilized fibrinogen ‘dot’ following blocking with Tris, a peeling effect was noted. A peeling or cracking of the immobilized fibrinogen surface is undesirable because it results in uneven platelet adhesion and the cracked surface can become loose and peel away during flow. Both of these occurrences resulted in unreliable platelet adhesion measurements. The following steps were taken to optimize the surface preparation to prevent the peeling effect from happening. First, the effect of the 1 M Tris-blocking agent on the immobilized fibrinogen was investigated using all of the following as blocking agents: 1 M bovine serum albumin (BSA), 1 M glycine, 1 M Tris and water. The images in figure 3-1 of the fibrinogen ‘dots’ following blocking demonstrate that it is not the 1 M Tris which is causing the peeling of the immobilized fibrinogen dots, as they all continue to peel under the different blocking conditions.

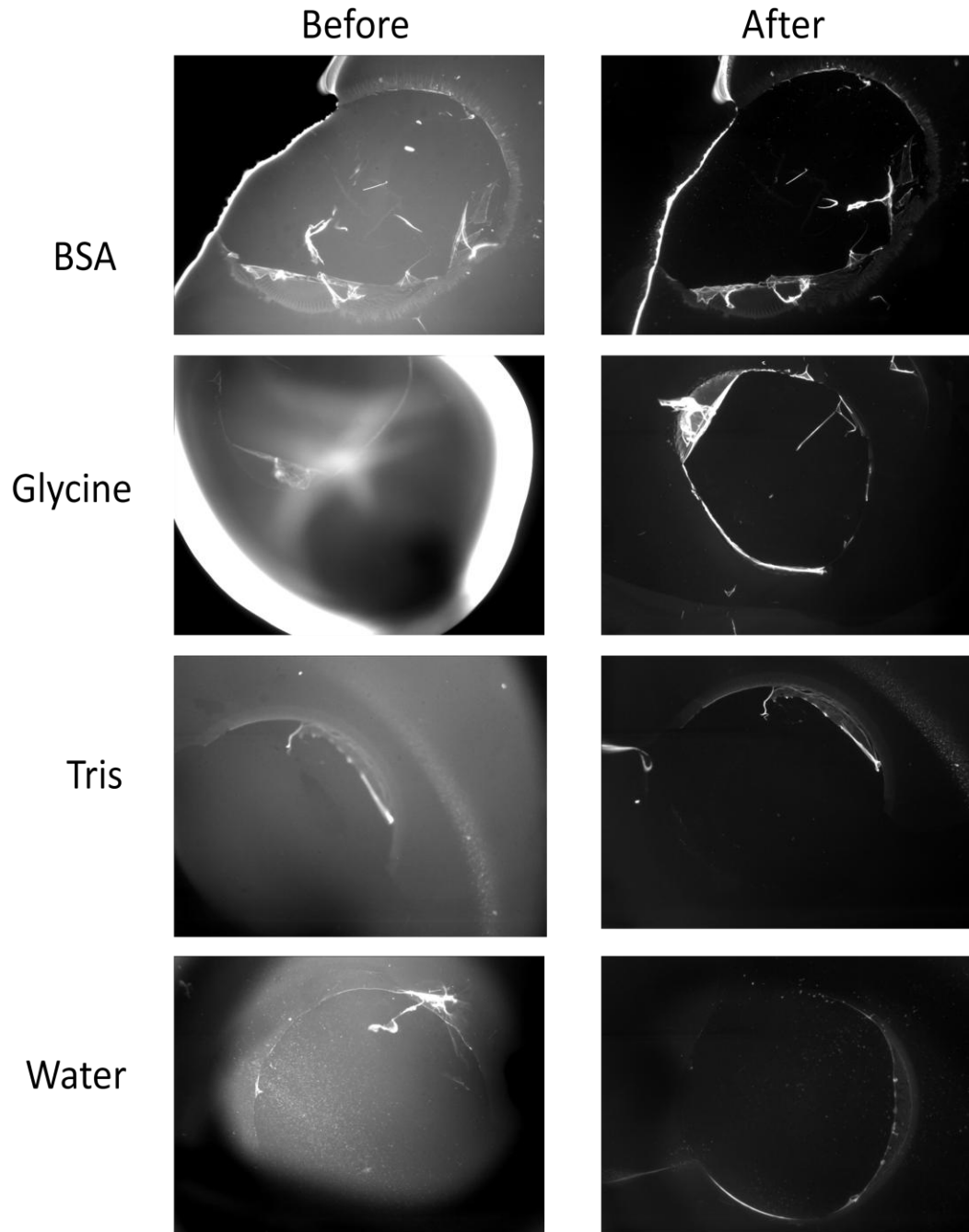


Figure 3-1 Variations in blocking agents do not affect fibrinogen dot peeling; the same extent of peeling is apparent for each type of blocking agent used, indicating the cause of peeling is not the process of blocking.

Chapter 3: Results

The next step undertaken to investigate the cause of the peeling effect was the surface chemistry responsible for tethering fibrinogen to the PDMS. Simultaneously, both the length of exposure in the plasma oxidation chamber and the percent volume of APTMES were varied. APTMES is soluble in ethanol, and the following percent volumes of APTMES in ethanol were used: 5%, 10%, 20%, and 50%. The length of exposure times in the plasma cleaner were varied as follows: 0 seconds, 20 seconds, 60 seconds (Fig 3-2); changing the length of exposure in the plasma cleaner effects the surface chemistry of the PDMS in the number of exposed functional groups.

The images in Fig 3-2 display the peeling effect that occurs at APTMES percentages above 5%, with increasing severity as the %APTMEs in ethanol increases (white arrows indicate sights of peeling). Upon visual inspection it is very clear that the preferred percent volume of APTMES in ethanol for use as a linker to immobilize fibrinogen on the surface of PDMS is 5%, as this percentage did not produce the peeling effect at any duration of plasma cleaning. It appeared that both the 60 second and 20 second plasma cleaning at 5% were effective; so the length of time used in experiments thereafter was 60 seconds due to the distinct border it produced. The 0 second exposure time appeared to produce a resilient fibrinogen dot, however the web-like extensions around the perimeter of each dot did not produce a distinct boundary, and it is not clear how this web would affect platelet adhesion or dynamics within the flow cell.

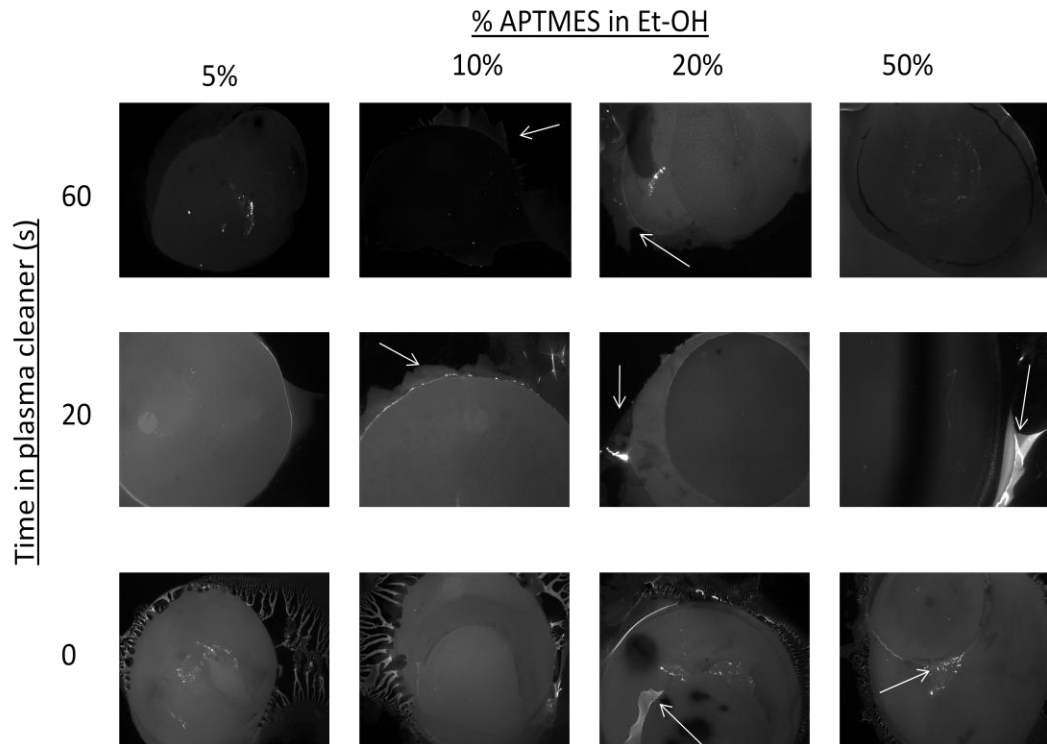


Figure 3-2 Images of FITC-fibrinogen immobilized on the surface of PDMS using varying lengths of plasma oxidation and varying percent volumes of APTMES in ethanol. The best combination of time in plasma oxidation and percent volume of APTMES in ethanol was 60 second and 5% because it produced no peeling and a distinct edge.

3.1.2 Labeling Platelets for Use in Flow Cell Experiments

Throughout the development of this technique, more than one compound has been assessed for efficiency, compatibility and an absence of interference with the cellular processes involved in platelet aggregation. Cell Tracker Green CMFDA dye was utilized to label isolated platelets, as the literature on the compound states that it does not adversely affect the processes involved in platelet aggregation. CMFDA has been previously shown to interact with intracellular thiols following free diffusion across the plasma membrane and transformation by esterases into a cell-impermeant fluorescent thioether dye (76). Baker *et al.* displayed the use of CMFDA in platelets for flow cytometry experiments, and claimed that the compound had no adverse effects on platelet aggregation processes (75); however, the opposite was observed when CMFDA was used in flow cell chamber experiments. Although platelet fluorescence was robust and long lasting, CMFDA appeared to stunt the ability of the platelets to adhere to immobilized fibrinogen. In figure 3-3 total adhesion, as a function of total fluorescence numbers, of platelets labeled with CMFDA was much lower than total adhesion of platelets labeled with Bodipy-FL. In figure 3-4 movie images taken from FITC and CMFDA labeled platelets shows the markedly reduced adhesion of platelets labeled with CMFDA dye.

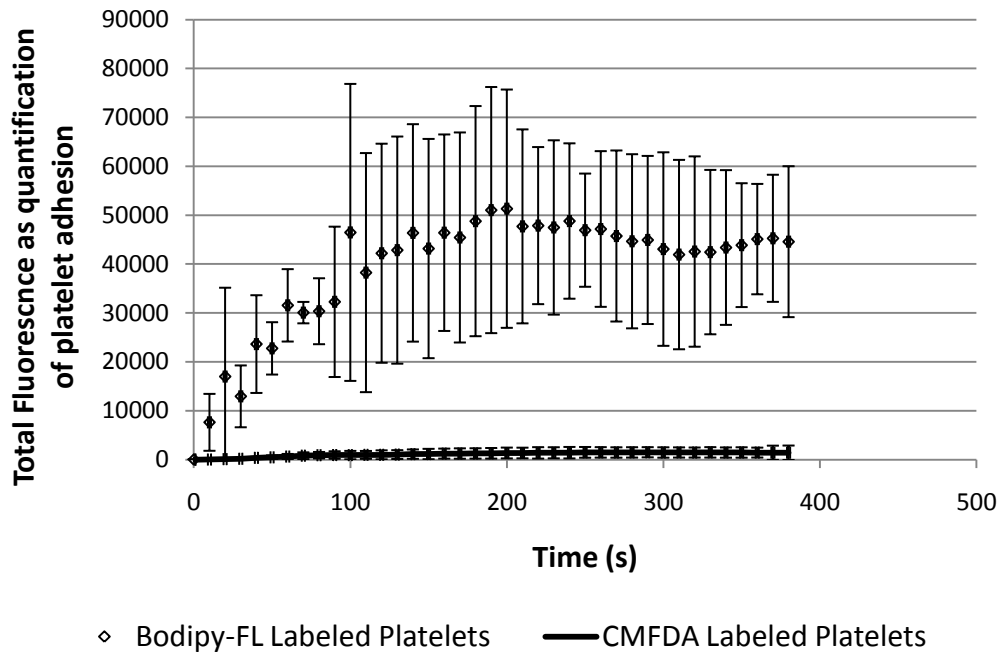


Figure 3-3 A comparison of the adhesion curves for platelets in flow cell chamber experiments run over immobilized fibrinogen. Platelets labeled with Cell Tracker Green CMFDA dye show inhibited ability to bind fibrinogen.

Chapter 3: Results

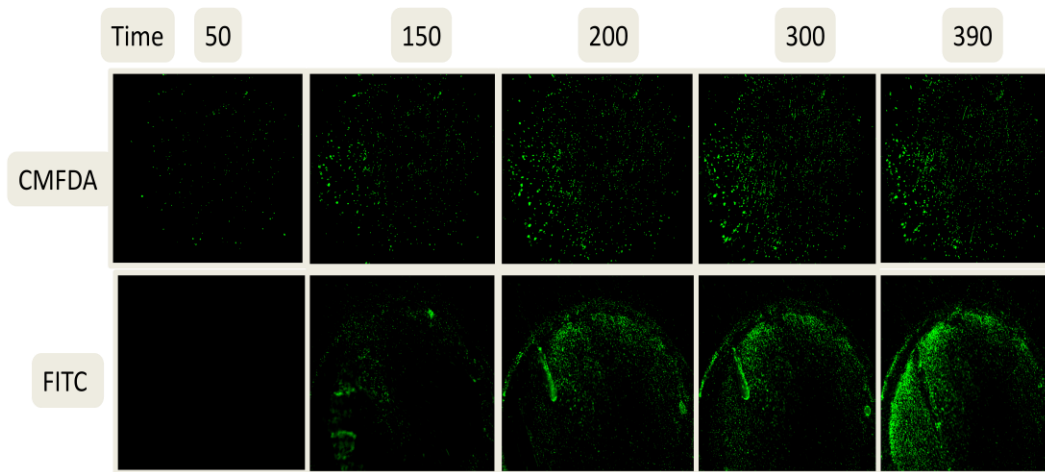


Figure 3-4 A comparison of images taken of the PDMS surface over the time course of a flow cell chamber experiment. Platelets labeled with CMFDA dye show markedly reduced ability to adhere to immobilized fibrinogen, while platelets labeled with FITC do not (time measured in seconds).

Chapter 3: Results

Although Bodipy-FL was used as a standard against which to compare the effectiveness of the CMFDA dye, it is not without its own complications. Bodipy-FL has been shown to be thiol reactive on the exofacial surface of the cell (77), which potentially interferes with integrin-mediated fibrinogen binding which, as previously discussed, has been shown to involve thiol disulfide bond shuffling. Thus, in an attempt to use a dye that is not thiol reactive on the extracellular or intracellular face, amine directed FITC was utilized. Unfortunately, FITC did not prove to be an effective solution for the platelet labeling problem. Upon initiation of the flow cell chamber experiment fluorescent light is shone at the sample every 10 seconds as it flows past the light source and microscope field of view. As a result, those platelets that adhere to the immobilized fibrinogen receive a dose of fluorescent light every 10 seconds from the time they adhere until the end of the run lasting a total of 390 seconds. Photobleaching due to exposure to fluorescent light was observed for FITC labeled platelets over the time course of the flow cell chamber experiment, shown in figure 3-5, that makes accurate platelet adhesion measurements impossible.

As a result of these investigations Bodipy-FL is the most effective platelet label for use in flow cell chamber experiments.

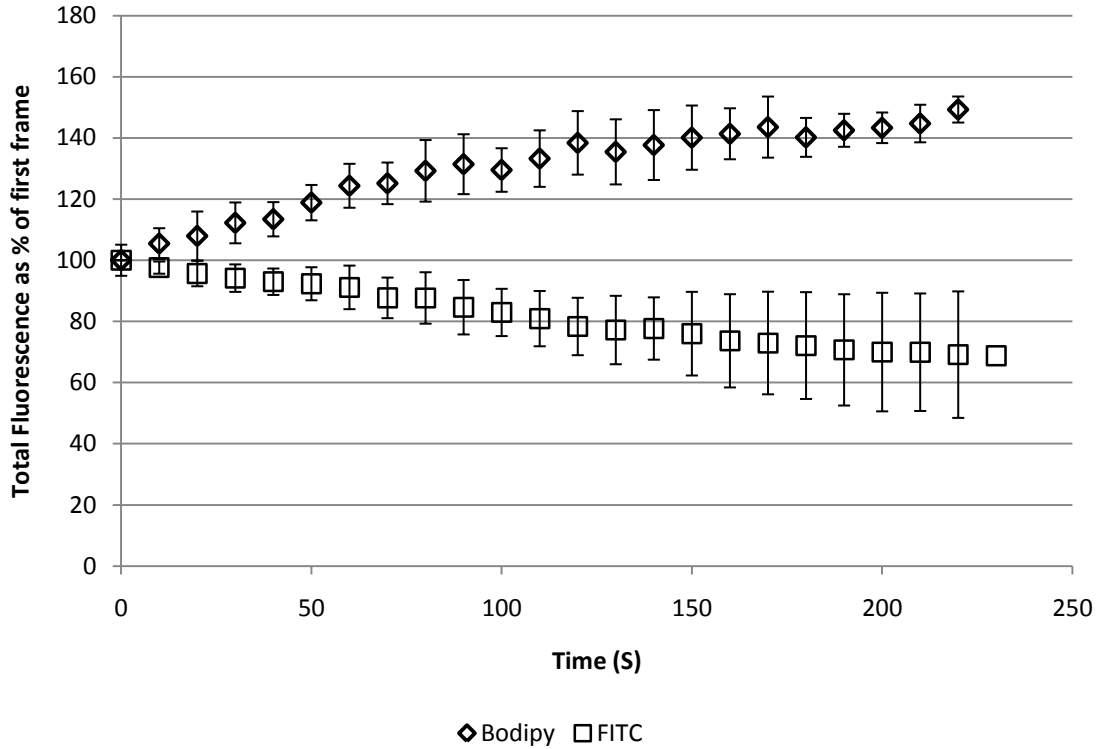


Figure 3-5 Photobleaching of platelets labeled with FITC compared to platelets labeled with Bodipy-FL. Over the time-course of the flow cell chamber experiment, it is clear that Bodipy-FL labeled platelets are able to reflect the increase in platelet adhesion, while the steady decline in fluorescence seen in FITC labeled platelets indicates a photobleaching effect of platelets adhered to immobilized fibrinogen (photobleaching shown as a percent of the adhesion value at the time decay begins; n=4).

3.2 Excess platelet surface proteins

In this study three proteins were assessed for their role and effects in platelet aggregation at the level of the cell surface: PDI, b-b' subunit of PDI and Hsp70. This analysis was done using a variety of techniques, one of which was turbidity assays performed by evaluating the extent of aggregation of platelets suspended in a cuvette as a measure of the decrease in turbidity within the cuvette over time. The second technique used to assess the effect of excess surface proteins on platelet aggregation was the flow cell chamber experiment, which allows the specific targeting of the protein of interest's role in the $\alpha_{2B}\beta_3$ integrin mediated platelet aggregation pathway. To deposit each protein in excess onto the surface of the platelet the law of mass action was utilized, and a high concentration of protein in solution was added to isolated platelets in suspension, tipping the equilibrium and causing deposition of protein on the platelet surface. Excess surface protein was verified by subjecting treated platelets to a 5% isopropanol wash; SDS-PAGE analysis of the wash supernatant (Fig 3-6) revealed more intense bands of the proteins of interest in treated platelets than in the native platelet isopropanol wash.

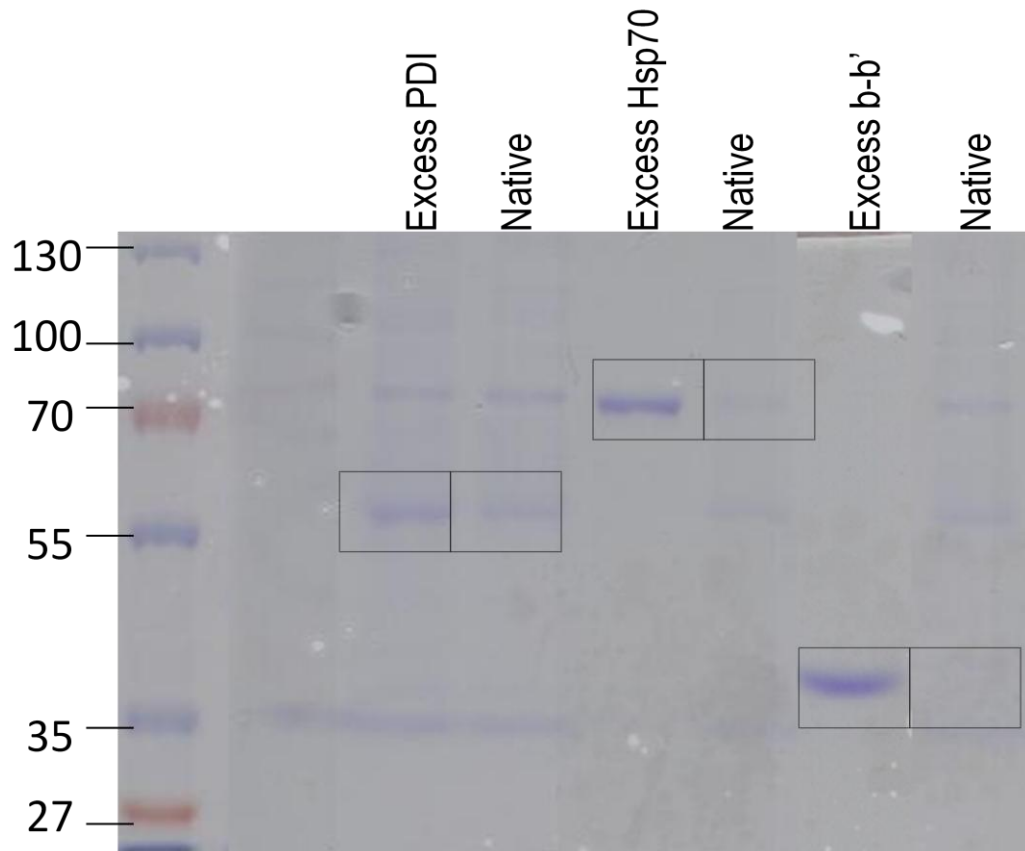


Figure 3-6 Platelets treated with excess protein of interest were subjected to a 5% isopropanol wash, and the wash was subjected to SDS-PAGE. The grey squares indicate where the law of mass action was successful in depositing excess amounts of protein onto the surface of the platelet. Using densitometry measurements in ImageJ the area under the curve was calculated to be (in order from left to right) 1276, 1156, 2191, 1229, 2741 and zero.

3.2.1 Investigation into the role of excess PDI on the platelet surface

There are many studies that assess the effect of PDI in platelet aggregation using RL90 anti-PDI antibody, the PDI inhibitor bacitracin and other competing substrates (47), all of which verify reliably that PDI has a role in platelet aggregation. The question that still remains unanswered is, what role PDI plays and in what pathway it participates in the complex aggregation process. In an attempt to further elucidate the role PDI is playing in platelet aggregation, excess PDI was deposited onto the surface of platelets via mass action to approach the investigation of PDI's role in platelet aggregation from a different angle. If PDI plays a role in a rate limiting step of the aggregation pathway, increasing platelet surface PDI would cause increased rates of aggregation which were assessed by both turbidity assays on the UV-VIS Spectrometer and platelet adhesions studied in the flow cell chamber experiments. Furthermore, by applying excess surface PDI to platelets in the flow cell chamber experiments, the potential role of PDI in the $\alpha_2\beta_3$ integrin mediated aggregation pathway will become clearer. PDI was deposited on to the surface of the platelet via mass action, and the presence of PDI on the surface was verified by imaging of labeled PDI on the surface (Fig 3-7). The effective labeling of PDI was verified by a fluorescence wavelength scan shown in figure 3-8, showing a peak at 540 nm with excitation at 520 nm for EITC labeled platelets (i), and a peak at 520nm with excitation at 488 nm for FITC labeled platelets (ii). In addition to the effects of the mere presence of PDI, the redox state of the deposited PDI was also investigated: PDI was induced into a reduced, oxidized or isomerization state and then incubated with isolated platelets.

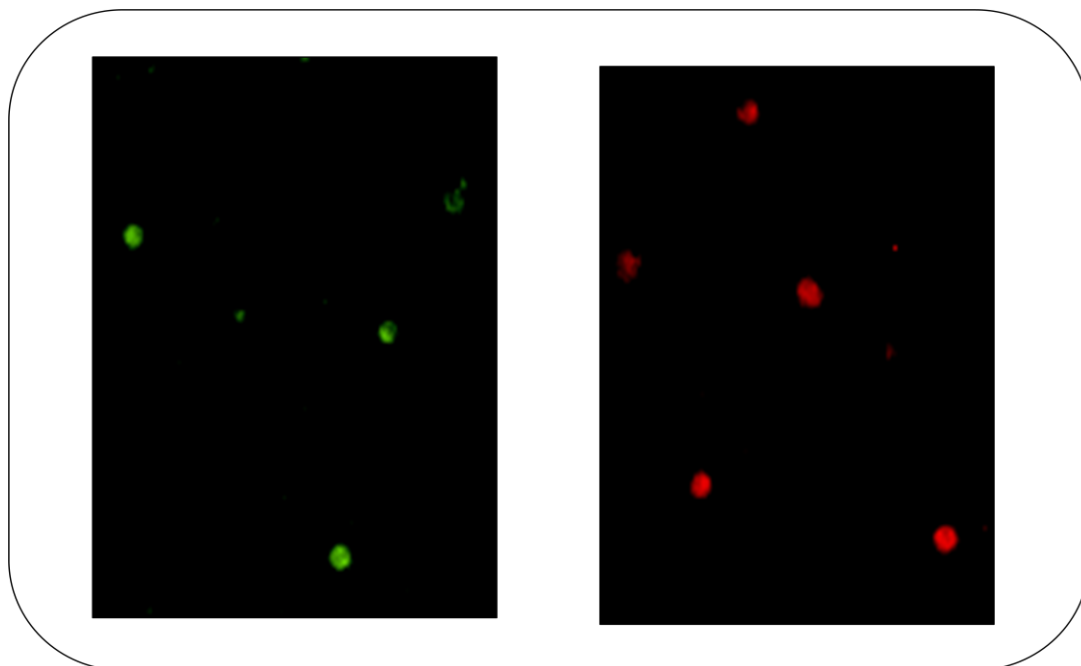


Figure 3-7 Verification of Mass Action deposition of redox modified or native state PDI onto the surface of isolated platelets. PDI is labeled with FITC (green) and EITC (red); the uniform colour verifies deposition onto the entire surface of the platelet.

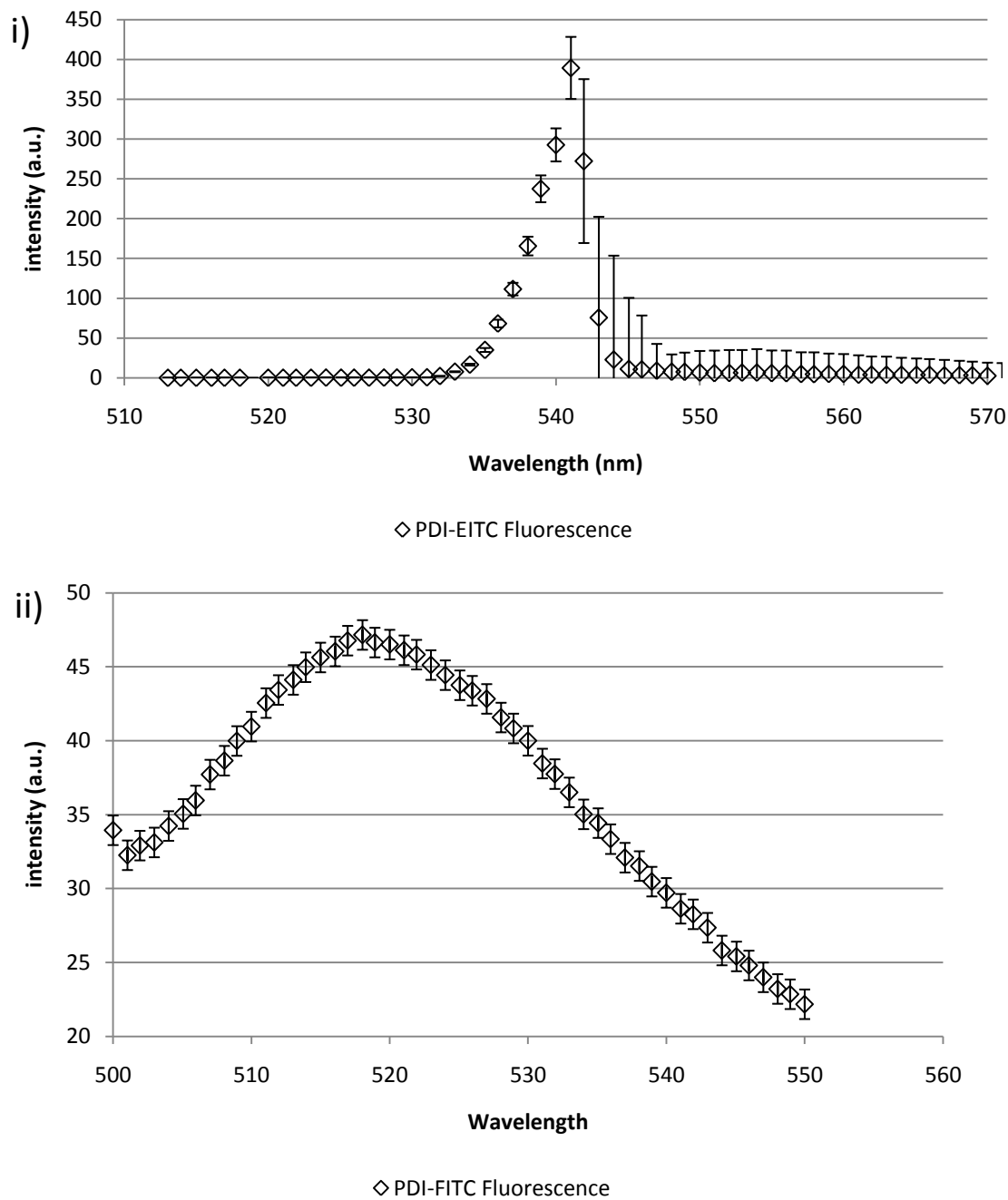


Figure 3-8 Fluorescence scan of i) EITC and ii) FITC labeled PDI, verifying the presence and fluorescence of the bound fluorophore

Chapter 3: Results

To verify the redox state of PDI, the Di-Eosin-GSSG assay (39) was utilized and the results are shown in figure 3-9. Oxidized PDI will not cleave Di-Eosin-GSSG and therefore will not produce an appreciable increase in emission fluorescence at 540 nm, however in a fully reduced state PDI will display very fast cleavage of Di-Eosin-GSSG and produce a large spike in emission. Hence, the ability to cleave GSSG is seen as a representation of oxidation state of the PDI molecule.

3.2.1.1 Turbidity Assay

To analyze the effect of excess PDI of various oxidation states on the aggregation rates of isolated platelets, turbidity experiments on the UV-VIS spectrometer were used to measure platelet aggregation. Figure 3-10 shows the combined results from all redox modified PDI platelet aggregations over different days using a variety of blood donors. The results from the turbidity assay aggregations imply that excess surface PDI had no significant effect on the initial rates of platelet aggregation, nor did the oxidation state of excess surface PDI appear to have any effect. From this general measure of platelet aggregation, PDI does not play a role in a rate limiting redox-dependent stage of the platelet aggregation pathway.

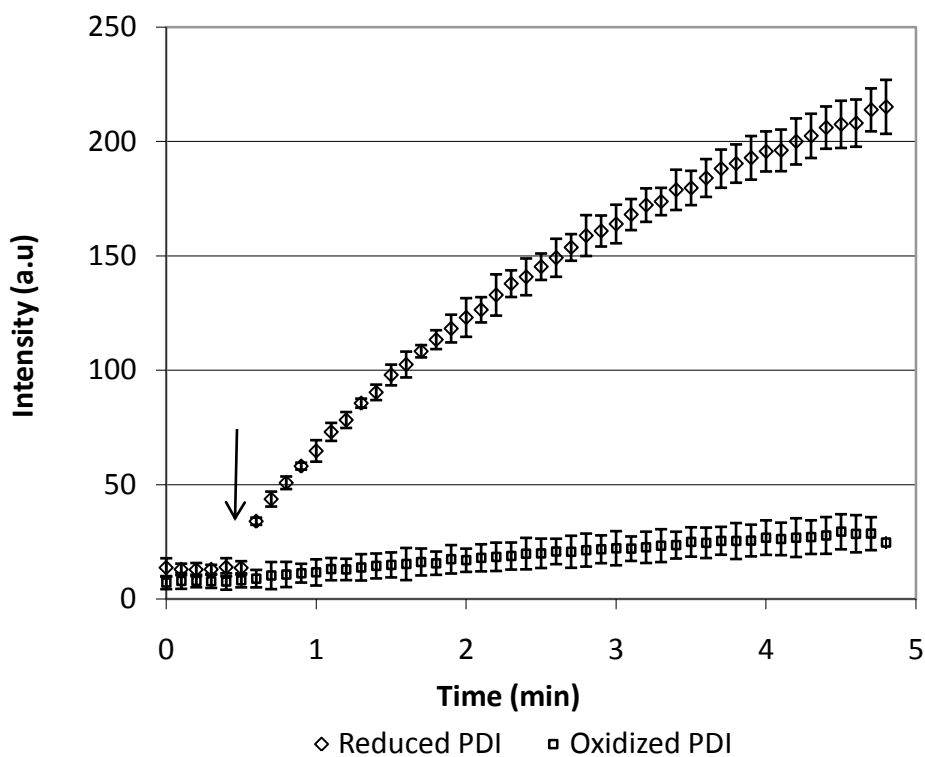


Figure 3-9 Verification of redox state of PDI by the Di-Eosin-GSSG Assay (@540 nm). Reduced PDI cleaves Di-Eosin at the GSSG disulfide, causing an increase in fluorescence. Oxidized PDI does not cleave the disulfides, thereby not producing an appreciable increase in fluorescence. Arrow indicates point at which PDI was added.

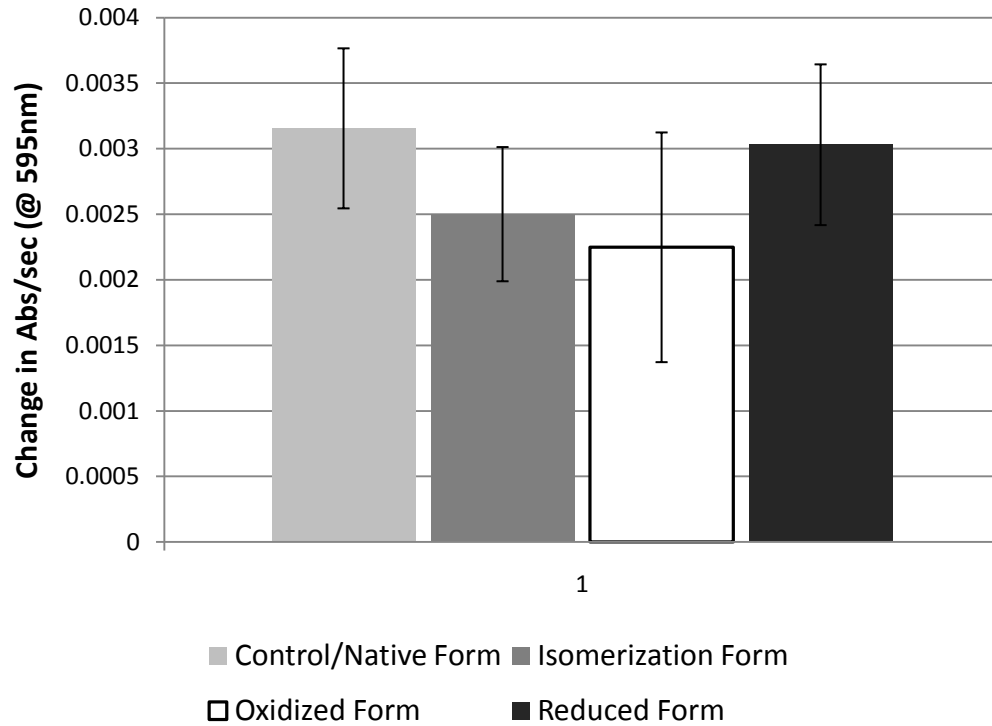


Figure 3-10 Initial rates of aggregation of isolated platelets incubated with PDI in various redox states; activated with 1 unit/mL thrombin, there is no significant difference in initial rates of aggregation between any of the treatments (n=31)

3.2.1.2 Aggregations Under Flow

To confirm the results seen in the spectrophotometer, platelet adhesion studies were done using flow cell chambers and whole blood utilizing the various treatments of PDI. Isolated platelets were either incubated with native PDI, oxidized PDI, reduced PDI or left in an untreated state, then recombined with whole blood to perform the experiment. The result of incubating isolated platelets with excess PDI at a concentration of 1 μM is shown in Fig 3-11. The results imply that incubating isolated platelets with excess PDI of native redox state had no influence on rates of adhesion of platelets to immobilized fibrinogen under flow conditions. This implication was confirmed by the theoretical total aggregation curves from the same experiment, wherein platelets treated with excess PDI achieved lower total aggregation than untreated platelets (Fig 3-12).

To verify the lack of effects on aggregation by redox induced PDI in the turbidity assays, the flow cell chamber experiment was utilized. For this investigation, three approaches were attempted: first, only reduced glutathione (GSH) or oxidized glutathione (GSSG) at concentrations of 7.2 mM and 0.72 mM respectively were added to the whole blood preparation 2 minutes before beginning the flow; second, isolated platelets were pre-incubated with redox-induced PDI prior to mixing with whole blood preparation; lastly, a combination of the two approaches was utilized with both pre-incubated platelets and GSH/GSSG added directly into the whole blood preparation. In all cases the results were inconclusive, with no statistical difference apparent between any of the treatment states (Fig 3-13).

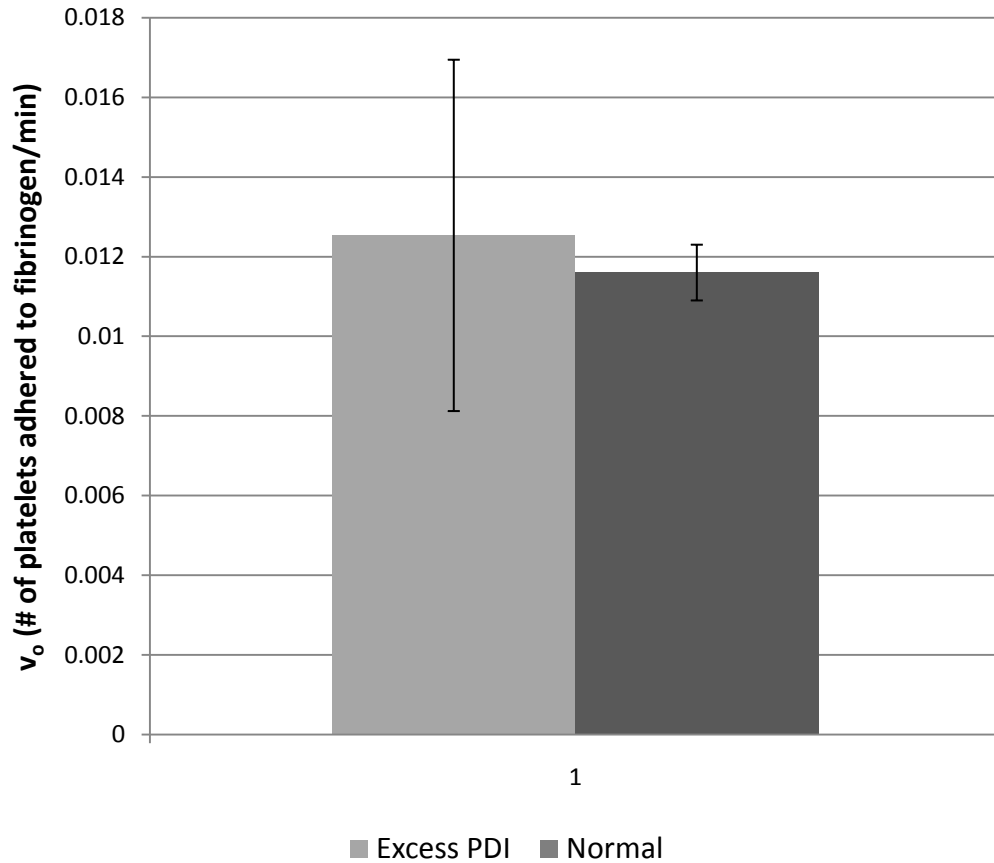


Figure 3-11 Average kinetics of platelet adhesion to immobilized fibrinogen under flow. Isolated platelets were pre-treated with or without excess PDI (1 μ M). There is no significant difference between adhesion rates with or without excess PDI (n=3).

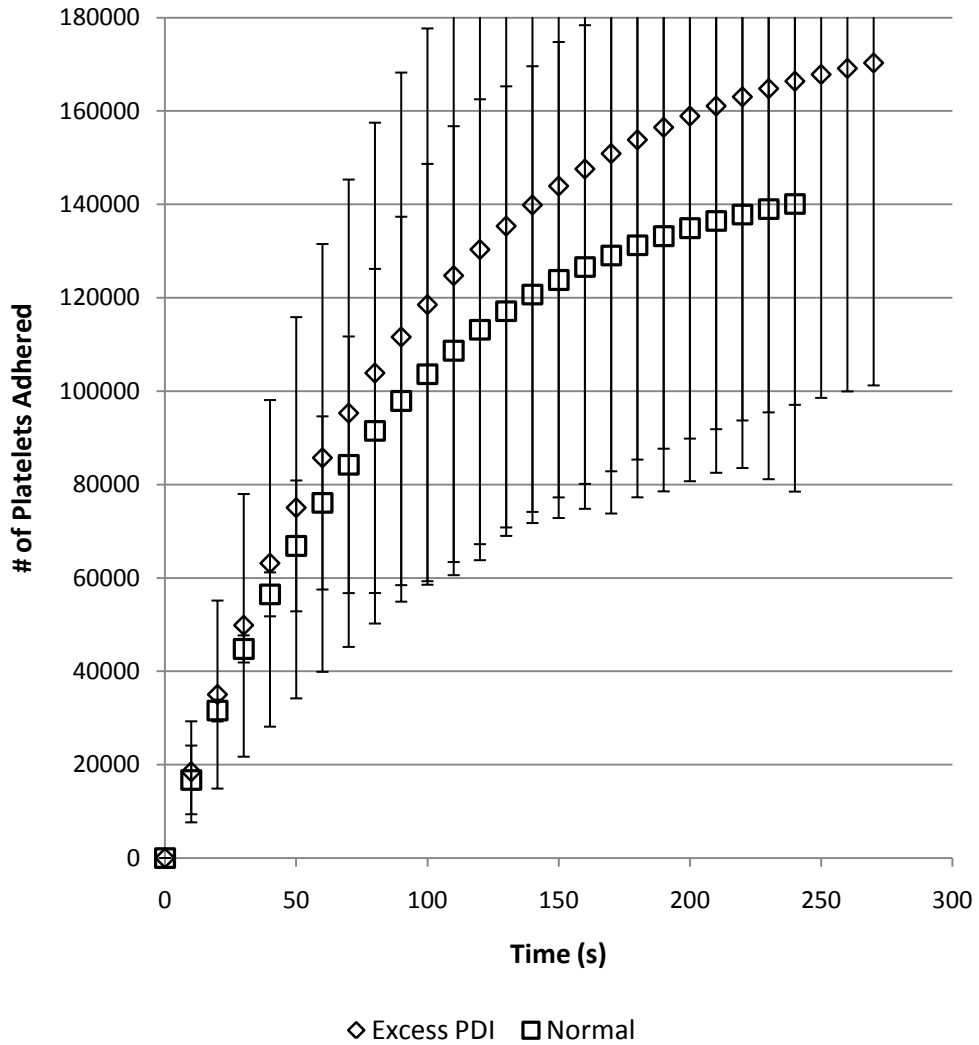


Figure 3-12 Total theoretical aggregation curves depicting platelet adhesion to immobilized fibrinogen under flow. Theoretical curves are constructed based on the initial rates of adhesion for each trial (n=3).

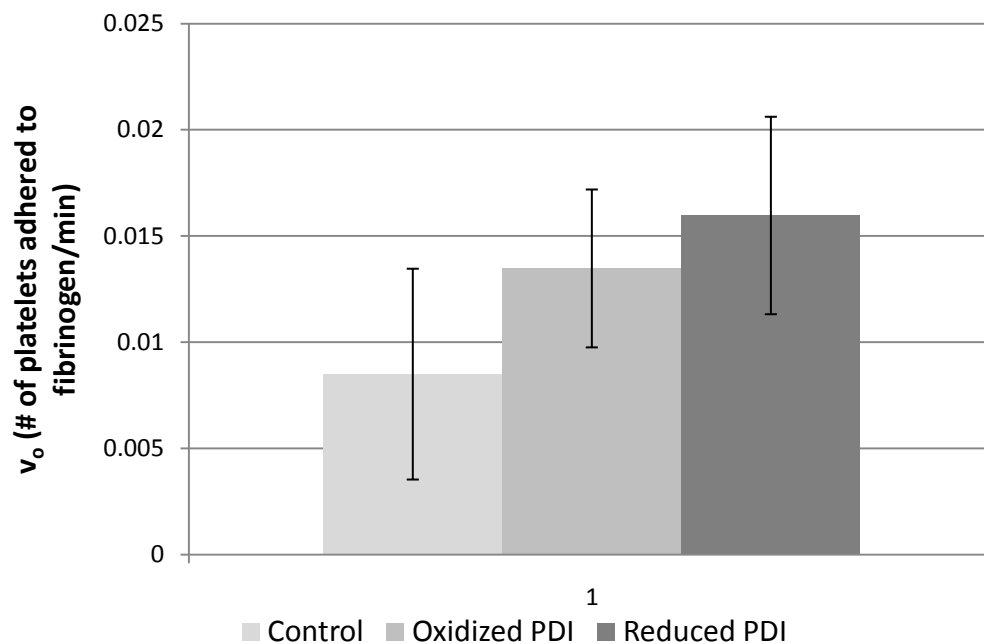


Figure 3-13 Kinetics of platelet adhesion to immobilized fibrinogen under flow when treated with reduced or oxidized PDI, GSH or GSSG. It was determined that there is no statistical difference between any of the treatment states.

Chapter 3: Results

In order to verify that the induced oxidation state in the flow cell chamber remains oxidized or reduced respectively throughout the entire experiment, plasma was isolated from the blood preparation and the concentration of free thiols was determined by 5,5'-Dithio-bis (2-nitrobenzoic acid) (DTNB) Assay. The DTNB assay confirmed that the induced redox state of the flow cell chamber preparation persists throughout the experiment (Fig 3-14).

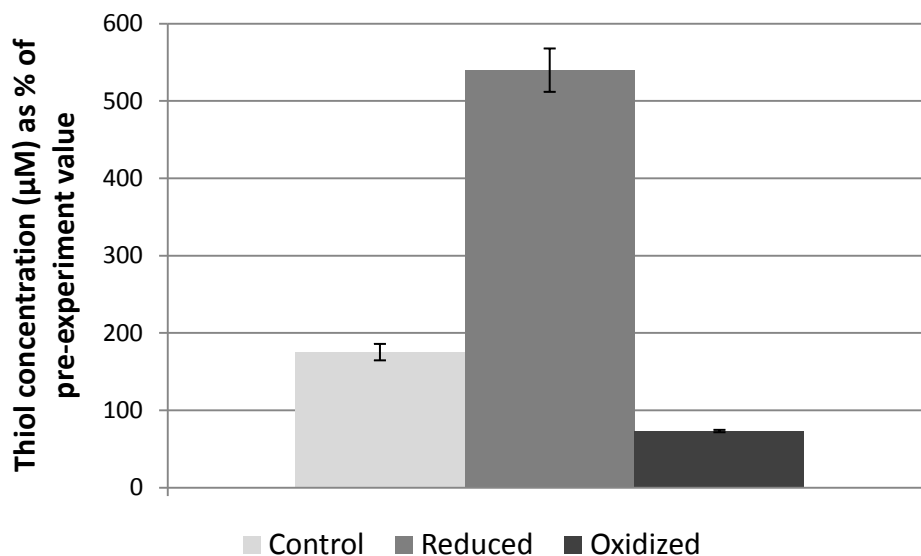


Figure 3-14 Concentration of free thiols in post flow plasma as a percent of the pre-experiment thiol concentration. The measured thiol concentration in plasma from the oxidized and reduced trials verifies that the redox state of the flow cell chamber environment remained oxidized and reduced respectively throughout the experiment.

3.2.2 Investigation into the role of excess b-b' subunit of PDI on the platelet surface

The **b-b'** subunits of PDI were of interest as possibly being the main effectors of PDI's documented augmentation of platelet aggregation. Since these subunits are responsible for proper protein positioning in the PDI catalytic cleft, there was speculation that they could exert a chaperone activity on platelet surface integrins, holding the $\alpha_{2B}\beta_3$ integrin in such a way to enable intrinsic disulfide isomerase activity (14) or isomerization by glutathione (78).

3.2.2.1 Turbidity Assay

Isolated platelets were activated with 1 unit/mL thrombin and aggregation was measured in the UV-VIS Spectrophotometer as a function of the change in turbidity of the sample. Initial rates of aggregation were compared between platelets treated with or without the **b-b'** subunits of PDI. Figure 3-15 shows the initial rates of aggregation between those platelets treated with **b-b'** and those left untreated are not significantly different; as a result the **b-b'** subunit of PDI does not appear to have its own chaperone function on the surface of platelets to potentiate aggregation.

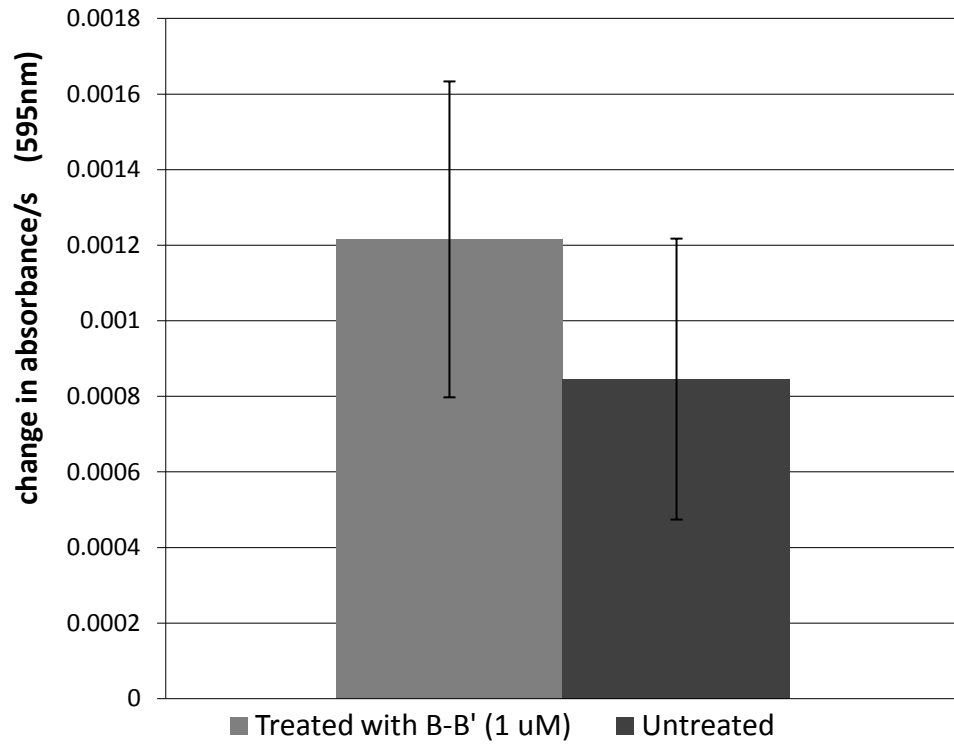


Figure 3-15 Initial rates of platelet aggregation following uncubation with 1 μ M b-b'. No statistical difference in the initial rates of aggregation was found between control and b-b' treated platelets (activated by thrombin (1 U/mL))

3.2.2.3 Aggregations Under Flow

To verify the effect of excess **b-b'** on the platelet surface in a physiologically relevant setting, isolated labeled platelets were re-introduced into whole blood and pumped over flow cell chambers containing immobilized fibrinogen. Following activation with calcium (4.6 mM), rates of adhesion are measured for all treatments (Fig 3-16). The turbidity assay results are confirmed by the more physiologically relevant flow cell chamber experiments and the chaperone-like role of the **b-b'** subunit of PDI in platelet aggregation is unsupported.

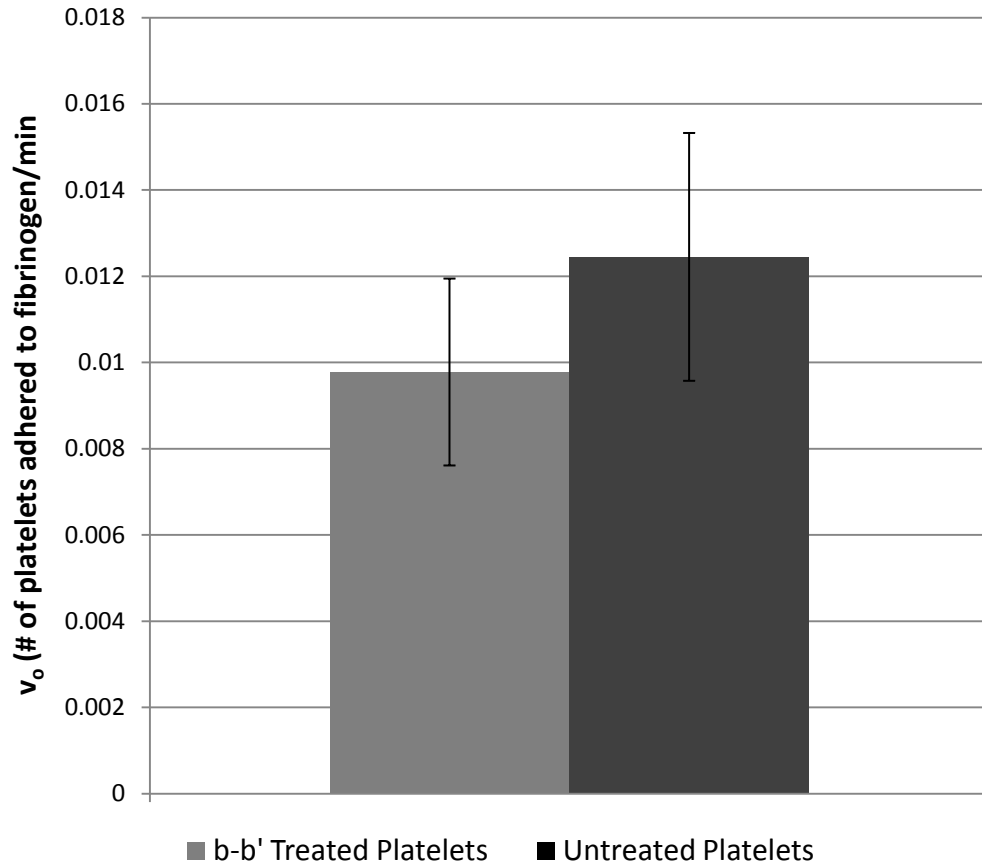


Figure 3-16 Average kinetics of b-b' treated platelet adhesion to immobilized fibrinogen under flow. There is no statistical difference found between treated and untreated platelets (n=5).

3.2.3 Hsp70 and its effects on platelet aggregation

During routine ethanol wash of the platelet surface, Hsp70 was identified on SDS-PAGE and Western blot (Fig 3-17); this was later confirmed by Suzanne Durocher in the Mutus Lab using gold nanoparticles to pull proteins off of the platelet surface (unpublished data).

3.2.3.1 The Effect of Hsp70 on platelet aggregation and adhesion under flow conditions

To test the potential role of cell surface Hsp70 in platelet aggregation, isolated platelets were incubated with Hsp70 prior to use in flow cell chamber experiments, much like the procedure used for PDI and the b-b' subunit. In addition, Hsp70 was added directly into the whole blood preparation prior to commencement of the flow cell chamber experiment. In both cases the results were the same, with Hsp70 treated platelets having no significant difference in initial rates of adhesion from native platelets (Fig 3-18). Figure 3-19 shows the images captured from various time points during the flow cell chamber experiment with excess Hsp70 on the surface of the platelet, confirming that there was no significant difference in platelet adhesion when excess Hsp70 was present on the platelet surface.

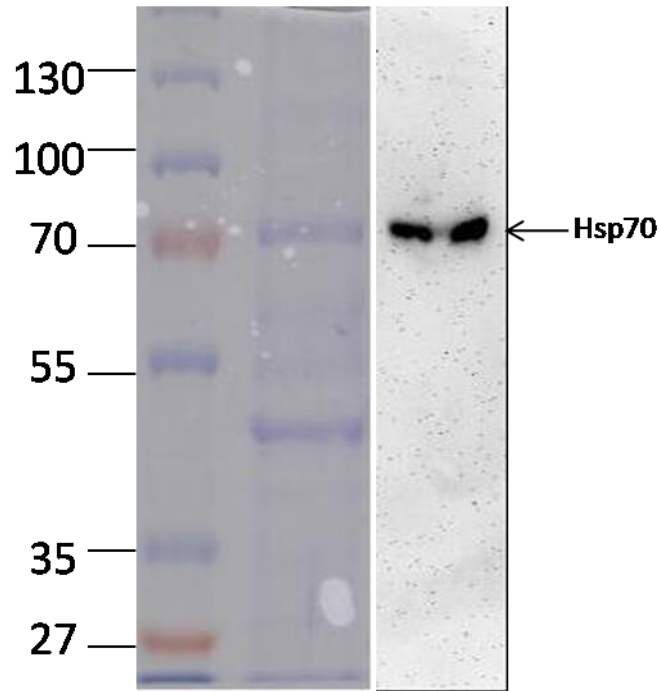


Figure 3-17 SDS-PAGE and western blot analysis of isolated platelet ethanol wash, identifying Hsp70 on the surface of the isolated platelet.

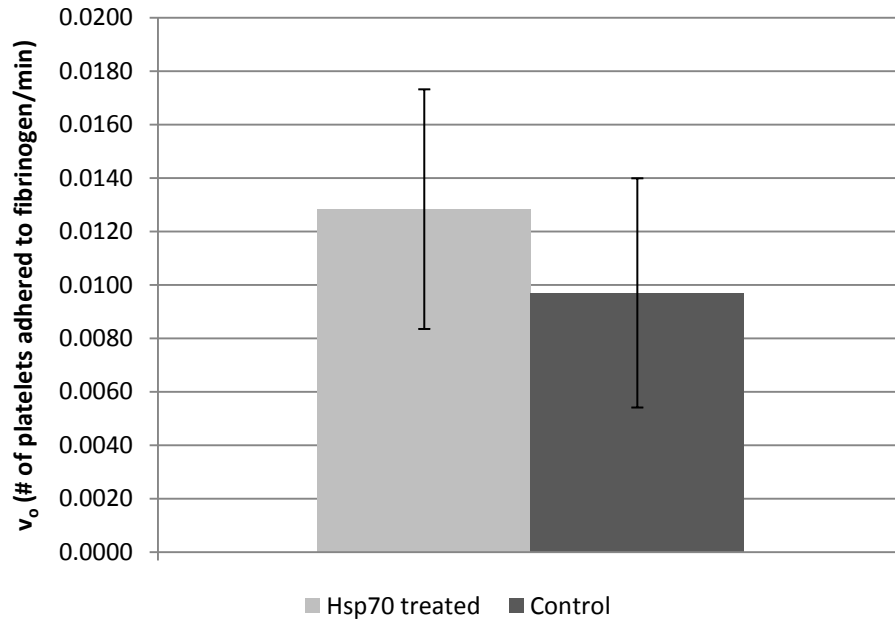


Figure 3-18 Kinetics of Hsp70 treated platelet adhesion to immobilized fibrinogen by activated platelets. No difference was found between Hsp70 treated and untreated platelets.

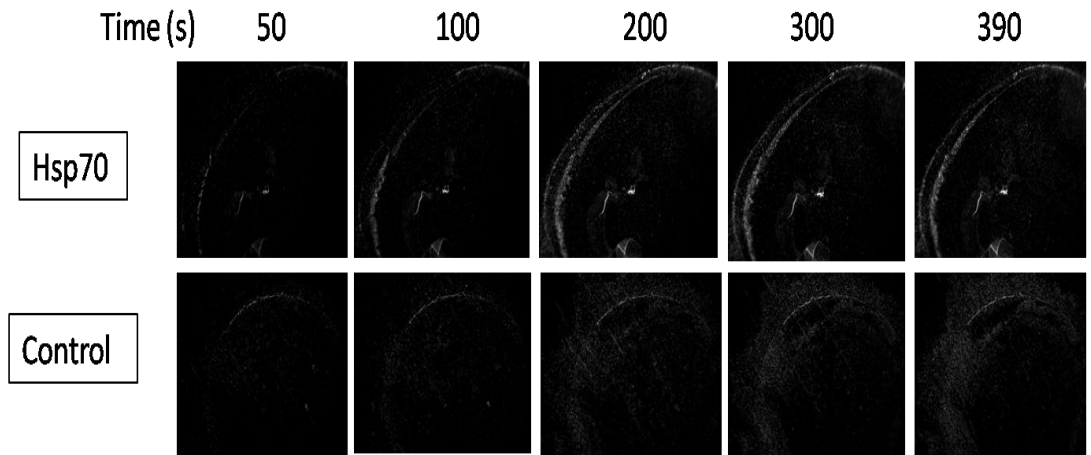


Figure 3-19 Images from a flow cell chamber experiment depicting the progression of adhesion of Bodipy-FL labeled platelets to immobilized fibrinogen, when pre-treated with Hsp70 or left in their native state.

3.3 Thymosin Beta Four

The effect of T β_4 on platelet aggregation is a question that holds much promise and potential. T β_4 has been revealed to possess remarkable healing powers on the skin and eye (58, 63), however a hypothesis was developed implicating elevated levels of T β_4 in diabetics and linking that to the elevated frequency of thrombotic events in persons with diabetes. The turbidity assay and flow cell chamber experiment were implemented to test the effect of varying doses of T β_4 on platelet aggregation and adhesion.

3.3.1 Turbidity Assay

Initially the effect of T β_4 on platelet aggregation was assessed using turbidity assays in the UV-VIS Spectrophotometer. At varying physiologically relevant doses of T β_4 (1 $\mu\text{g/mL}$ to 100 $\mu\text{g/mL}$) the extent and initial rate of platelet aggregation was assessed as a function of decreased absorbance. Figure 3-20 shows that T β_4 influenced platelet aggregation at some doses, while having no effect at other doses. At 1 $\mu\text{g/mL}$ T β_4 appeared to slightly increase the initial rate of aggregation, however at 5 $\mu\text{g/mL}$ and 10 $\mu\text{g/mL}$ there was a significant increase in initial rate of platelet aggregation over control. As the concentration of T β_4 continued to increase, the positive effect on rate of aggregation diminished, and by 50 $\mu\text{g/mL}$ the initial rates of aggregation were back to control levels.

Chapter 3: Results

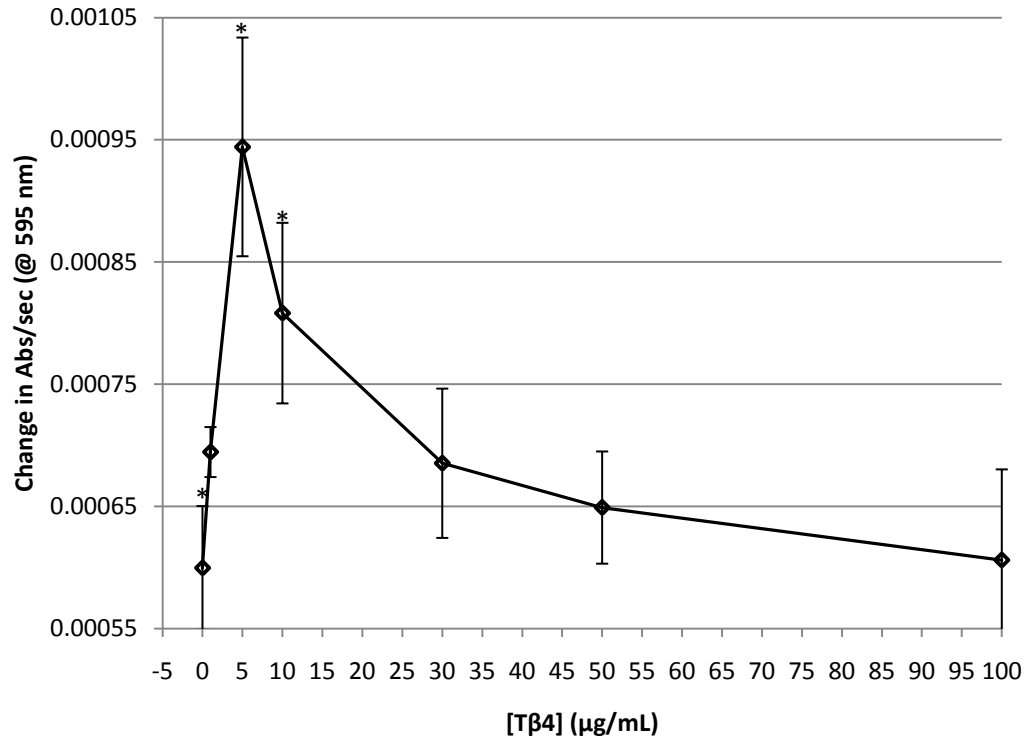


Figure 3-20 Initial rates of aggregation of platelets treated with varying doses of TB4 in the turbidity assay (* = significant difference when $P < 0.05$; $n=5$)

3.3.2 The effect of $T\beta_4$ on platelet adhesion under flow conditions

To investigate the effects of $T\beta_4$ on platelet aggregation in a more physiologically relevant experimental setting, $T\beta_4$ was added at varying doses to the whole blood preparation prior to the onset of the flow cell chamber experiment. In the flow cell chamber experiment, the same positive effect on platelet aggregation was seen in figure 3-21 for $T\beta_4$ doses of 1 $\mu\text{g}/\text{mL}$ and 5 $\mu\text{g}/\text{mL}$; however, the 10 $\mu\text{g}/\text{mL}$ dose did not appear to have the same effect as it did in the turbidity assay. As observed previously, as the dose of $T\beta_4$ increased above 10 $\mu\text{g}/\text{mL}$, the positive effect on platelet aggregation diminished back toward control levels.

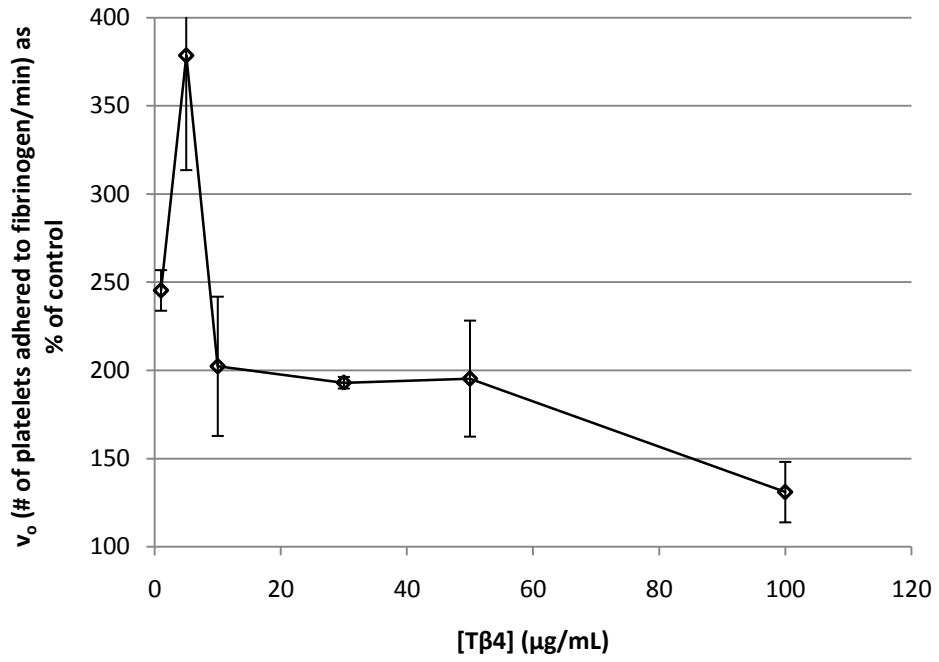


Figure 3-21 Kinetics of platelet adhesion to immobilized fibrinogen under flow conditions at varying doses of TB4 (n=3)

3.3.3 Fibrinogen Binding of T β ₄

Since the main platelet activation pathway targeted by the flow cell chamber experiments is the $\alpha_{2B}\beta_3$ integrin pathway, which acts as a fibrinogen binding receptor (79), T β_4 was tested to determine whether it was diminishing platelet aggregation at high doses by binding to fibrinogen, thereby preventing platelet adhesion. Figure 3-22 shows the curve of FITC labeled T β_4 binding to PDMS immobilized fibrinogen in a 96 well plate. As the concentration of T β_4 increases beyond 30 $\mu\text{g/mL}$, the binding of T β_4 to fibrinogen begins to diminish as well; this points to T β_4 not as an inhibitor of platelet aggregation at high concentrations, but rather as a switch acting to potentiate platelet aggregation rates at intermediate doses, while releasing from fibrinogen at high doses and allowing aggregation to occur at normal levels.

The effect of T β_4 -fibrinogen binding on platelet aggregation was investigated in the spectrophotometer to confirm the hypothesis that intermediate doses of T β_4 caused elevated initial rates of platelet aggregation. Figure 3-23 shows the initial rates of aggregation as a percentage of control, and clearly shows that at the T β_4 concentrations between 1 $\mu\text{g/mL}$ and 10 $\mu\text{g/mL}$ with fibrinogen present the rates of aggregation were lower than those without fibrinogen present; however at 30 $\mu\text{g/mL}$ and 50 $\mu\text{g/mL}$ the initial rates of aggregation converge. Therefore it appeared that T β_4 bound to free fibrinogen in the cuvette at intermediate doses, preventing the previously seen peak in initial rates of aggregation at 5 $\mu\text{g/mL}$. When fibrinogen was immobilized in the flow cell chamber experiment, or absent in the cuvette, free T β_4 was available for interaction with the platelet and augmentation of adhesion and aggregation.

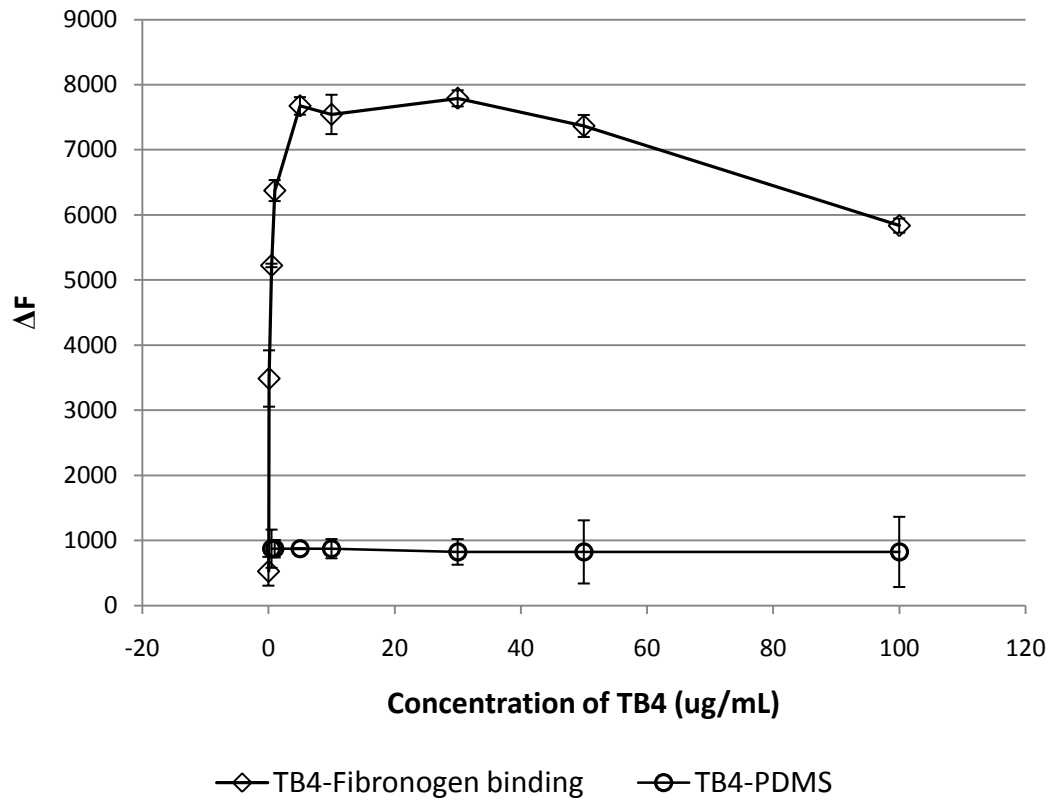


Figure 3-22 Tβ4- fibrinogen binding curve. Fibrinogen was immobilized on PDMS in a 96-well plate while EITC labeled Tβ4 was added at varying doses. The resultant binding curve displays a relationship akin to first order kinetics, excepting the decrease in binding that occurs above [TB4] of 30 μg/mL (n=4).

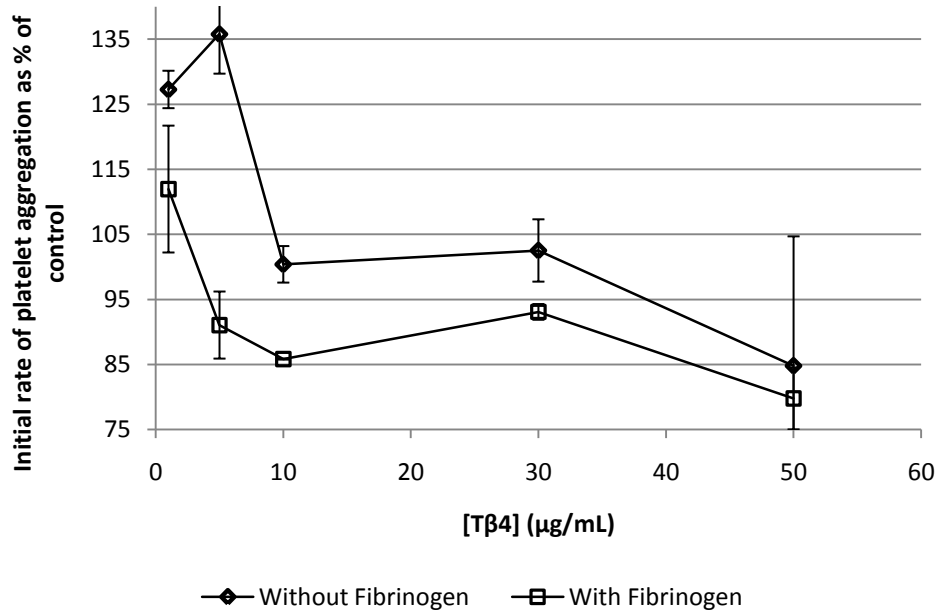


Figure 3-23 Initial rates of aggregation of platelets in a turbidity assay shown as a percent of control. Platelet aggregation was measured in the presence or absence of TB4 and fibrinogen. A peak at [TB4] 5 µg/mL correlates with the strong binding seen in the TB4-fibrinogen binding curve; in the presence of fibrinogen this peak in aggregation disappears (n=4).

Chapter 4 DISCUSSION

4.1 Flow Cell Methodology Development

In this study, the development of the flow cell chamber methodology was a focus in order to establish the method as a reliable and efficient tool for evaluating platelet adhesion under many conditions. The eventual goal is to use the method diagnostically to assess platelet adhesion and aggregation in persons with bleeding disorders to determine the exact receptor, signaling molecule or pathway that is responsible for the problem. Some difficulties encountered while working extensively with this method include bound platelet imaging problems; continuity of results between runs, between sessions and between blood sources; cracking and peeling of immobilized fibrinogen on PDMS causing unreliable adhesion counts; and clogging of the flow cell apparatus during runs. The issue of bound platelet imaging is a difficult one to solve, mainly because the problem is that those platelets passing by the field of view at the moment the image is captured may not be stuck to the PDMS. As a result the platelet adhesion count may be confounded by those platelets floating above the PDMS surface that are also captured in the image. Although the flow rate is constant, this does not necessarily mean that the number of platelets passing by the field of view every second is the same—bubbles and currents that form in the chamber cause surges of platelet numbers at random times. The ideal solution would be to find or make a fluorophore that becomes fluorescent *after* platelet adhesion to the protein matrix takes place; this is a very challenging concept, but perhaps enough knowledge about the receptor utilized to bind to the protein matrix, and

Chapter 4: Discussion

Careful targeted labeling of that receptor, could allow this concept to be realized. Naturally if only bound platelets are emitting light, any issue with unbound platelets confounding fluorescent measurements would be eliminated. Of the fluorescent labels assessed in this study, the most efficient and effective dye that does not display any inhibitory effects on platelet aggregation or fibrinogen-mediated platelet adhesion, is the Bodipy-FL fluorescent dye. Although it is an exofacial thiol targeted dye, it appears that the thiols within the $\alpha_{2B} \beta_3$, which are necessary for proper inside-out signaling to commence, are unaffected by this dye.

The issue of continuity of results is a frustrating problem and although the trends are similar, the raw platelet adhesion numbers are always different from experiment to experiment, and sometimes can vary widely. The same can be said for trials done within one experiment, with variations in the total adhesion numbers unexplainable by any of the methodology used in the experiment, as each trial is treated exactly the same as the one before and the one following, with controlled cell counts. So although trends can be teased out, the error bars prevent significant statistical analysis of the data. A potential solution to this problem remains evasive, as the only possible source of the problem would appear to be the methodology; however with each and every trial treated exactly the same, it becomes difficult to pinpoint the cause of this issue.

The clogging of the flow cell apparatus is an indicator of both success and problems. It indicates success because of the physiological relevance of the thrombosis occurring within the tubes, confirming that this method is very close to the process within the vessels of the body. However, continuous clogging of the apparatus wastes blood and plasma stores, and it makes that chamber and that trial a waste as well. Sometimes a

Chapter 4: Discussion

manipulation of a variable substantially increases platelet aggregability, but it leads to clogging of the apparatus before fibrinogen binding can be quantified. Perhaps the small volume of blood that is continuously circulated causes thrombosis at such an elevated and perpetuated level upon addition of the calcium, that aggregation and thrombus formation occurs out of normal physiological levels. Ideally a larger blood volume would be circulated, which requires access to very large volumes of fresh blood to allow for the number of trials that will be necessary to satisfy error. Perhaps even direct circulation from a sedated animal to the chamber would provide the most physiologically relevant results.

The issue of cracking and peeling of the immobilized fibrinogen dot was solvable, and the results are displayed in section 3.1.1. Visually, it appeared that at concentrations of APTMES in ethanol higher than 5%, a dome-like APTMES dot formed. With a dome shape, addition of any liquid substance at the apex of the dome—such as fibrinogen and BS_3 --resulted in gravitational movement of the liquid down the sides of the dome and deposition in a ring surrounding the dome. Some fibrinogen became bound to BS_3 on the surface of the APTMES dome, however the APTMES at the apex of the dome must not have covalently linked to the exposed functional groups on the surface of the PDMS due to simple distance restrictions. Therefore, the lack of covalent bonds between PDMS and the apex of the APTMES dome resulted in cracking and peeling of the dome upon addition of shear stress. At APTMES concentrations of 5% or lower, the dome shape did not form—a spreading effect took place when the APTMES was applied to the surface of the PDMS. The high ethanol content reduced the surface tension of the APTMES component, allowing the rapid spreading to occur and eliminating the production of a

'dome; ethanol evaporated from the surface of the PDMS, leaving the PDMS-APTMS complex behind. The downfall to this approach is that the area coated with fibrinogen is large: usually this area is larger than the field of view at 5x magnification, and as a result seeing platelet adhesion to the entire fibrinogen-coated area is not possible.

4.2 Surface deposition of b-b', PDI and Hsp70 and their effect on platelet aggregation

In this study the effects of excess surface PDI, Hsp70 and the b-b' subunit of PDI were investigated. Excess surface protein was deposited on the platelet exofacial membrane through mass action deposition, and was verified by fluorescence microscopy. Experiments were performed on the treated platelets in the UV-VIS Spectrometer and on flow cell chamber apparatus, to determine if the excess surface protein had an effect on initial rates and extent of platelet aggregation. There remains some question as to whether depositing excess protein on the surface of a cell should potentiate the aggregation response or not; it has been documented in the literature that PDI has an effect on platelet aggregation (47), and yet excess surface PDI did not cause significantly faster platelet aggregation. So, perhaps more protein did not equate to a faster response, possibly due to the rate limiting step of the platelet reaction being upstream of the surface protein. Given the increased levels of surface protein verified in figure 3-2, it follows that the excess protein was not internalized or cleaved; however, it is also possible that although the protein had been effectively deposited on the surface of the protein, that it was not being integrated into the network of effectors on the platelet surface that work

Chapter 4: Discussion

together and with synchronicity in order to realize the platelet reaction of aggregation and adhesion. To combat these issues in the future it would be ideal to find ways of treating platelets to instigate upregulation of the proteins of interest, thereby making them completely native to the cell and integrated into the complex aggregation pathway. Furthermore, as many researchers have done in the past (47, 80-81), utilizing specific receptor antagonists to block or alter the proteins of interest would be another way to confirm the real-time effect of the protein of interest on platelet aggregation and adhesion. While none of the effects of excess surface protein on platelet aggregation were statistically significant, the trends do reliably exist. To be conclusive with these results smaller error bars would be required, and the ideas and suggestions outlined in section 4.1 would certainly help towards making that objective possible. Additionally, due to the highly sensitive nature of platelets, very strict use of only one individual's platelets taken at the same time of day, using the platelets the same length of time after being drawn, and doing enough trials at a time to be able to deduce statistically reliable results from one day's experiments, would also help to reduce the error bars.

4.3 Thymosin β_4

In this study, T β_4 was investigated to determine if elevated levels caused increased rates of platelet aggregation and adhesion. In the clinical setting patients with diabetes mellitus have been shown to suffer from clotting in the extremities causing lower body circulation problems, sometimes even resulting in foot or leg amputation. Working with a hypothesis that elevated blood levels of T β_4 could be contributing to the higher clotting

Chapter 4: Discussion

potential of diabetics, the presence of excess levels of $T\beta_4$ was evaluated for effects on platelet aggregation in both the turbidity assays on the UV-VIS Spectrophotometer, and the whole blood flow cell chamber experiments. In both cases, $T\beta_4$ produced measurable results on platelet aggregation, with the most significant potentiating effects on platelet aggregation seen at 5 $\mu\text{g/mL}$; at much higher doses of $T\beta_4$, the trend of potentiation disappeared. To elucidate what could possibly be causing the trend to rise at intermediate levels of $T\beta_4$ but diminish at higher levels of $T\beta_4$, the relationship of $T\beta_4$ with fibrinogen was analyzed. Thymosin β_4 was found to bind to PDMS-immobilized fibrinogen with a relationship akin to first-order kinetics (figure 3-22); as a result there was a direct relationship between the amount of $T\beta_4$ -fibrinogen binding and the concentration of $T\beta_4$ up to saturation at 30 $\mu\text{g/mL}$, with an estimated dissociation constant (K_d) of 25 nM. Beyond that saturation point, the extent of fibrinogen binding began to decrease, implying that beyond the saturation point $T\beta_4$ was off-loading from fibrinogen. This corroborates the trend seen in the turbidity and flow cell chamber data, where at intermediate concentrations of $T\beta_4$ the effect on rate of platelet aggregation/adhesion was potentiating, however at higher concentrations of $T\beta_4$ the effect on rate of platelet aggregation/adhesion was almost absent, resulting in rate levels very close to control. To further corroborate this finding, platelet aggregations were performed in the UV-VIS Spectrophotometer with or without fibrinogen present, at varying doses of $T\beta_4$. A very intriguing trend was produced in this experiment: at lower doses of $T\beta_4$, the peak in rate of platelet aggregation at 5 $\mu\text{g/mL}$ disappeared with fibrinogen present, but the peak was present in the absence of fibrinogen. Beyond $T\beta_4$ concentrations of 10 $\mu\text{g/mL}$ the rates of aggregation began to mirror each other, with rates in the presence of fibrinogen

Chapter 4: Discussion

approximately 5% lower than rates in the absence of fibrinogen. Knowing that $T\beta_4$ binds fibrinogen most effectively between the concentrations of 5 and 30 $\mu\text{g/mL}$ and taking into account the very narrow K_d of 25 nM, it is probable that free fibrinogen and free $T\beta_4$ were interacting in the cuvette above the $[T\beta_4]$ of 5 $\mu\text{g/mL}$, therefore sequestering it and preventing it from potentiating platelet aggregation. However, at $[T\beta_4]$ of 10 $\mu\text{g/mL}$ and above, the difference between the initial rates of platelet aggregation in the presence or absence of fibrinogen get sequentially smaller. So, why does the binding strength in the cuvette appear to weaken at 10 $\mu\text{g/mL}$, while in the 96-well plate the binding strength appears to remain resilient until beyond 30 $\mu\text{g/mL}$? One consideration to make is that upon exposure to thrombin, platelets release $T\beta_4$ in quantities of up to 6 fg/cell (61). The concentration of $T\beta_4$ indicated by the x-axis (figure 3-23) accounts for only the peptide added by experimental methods, not for any $T\beta_4$ that may have been released by platelets. As a result, the concentration of $T\beta_4$ may be higher than indicated on the x-axis when administered $T\beta_4$ is taken into account in addition with $T\beta_4$ released from platelets. Another possibility is that free fibrinogen binds $T\beta_4$ with different dynamics than immobilized fibrinogen due to a difference in steric constraints placed on fibrinogen while it is immobilized. Thus, fibrinogen may potentially become saturated at lower $T\beta_4$ concentrations when free in solution. The well known actin binding domain LKKTETQ (82) does not have a clear binding sequence on fibrinogen, however in figure 4-1 are areas of consensus sequence between fibrinogen and $T\beta_4$ where potential non-covalent interactions between fibrinogen and $T\beta_4$ could occur.

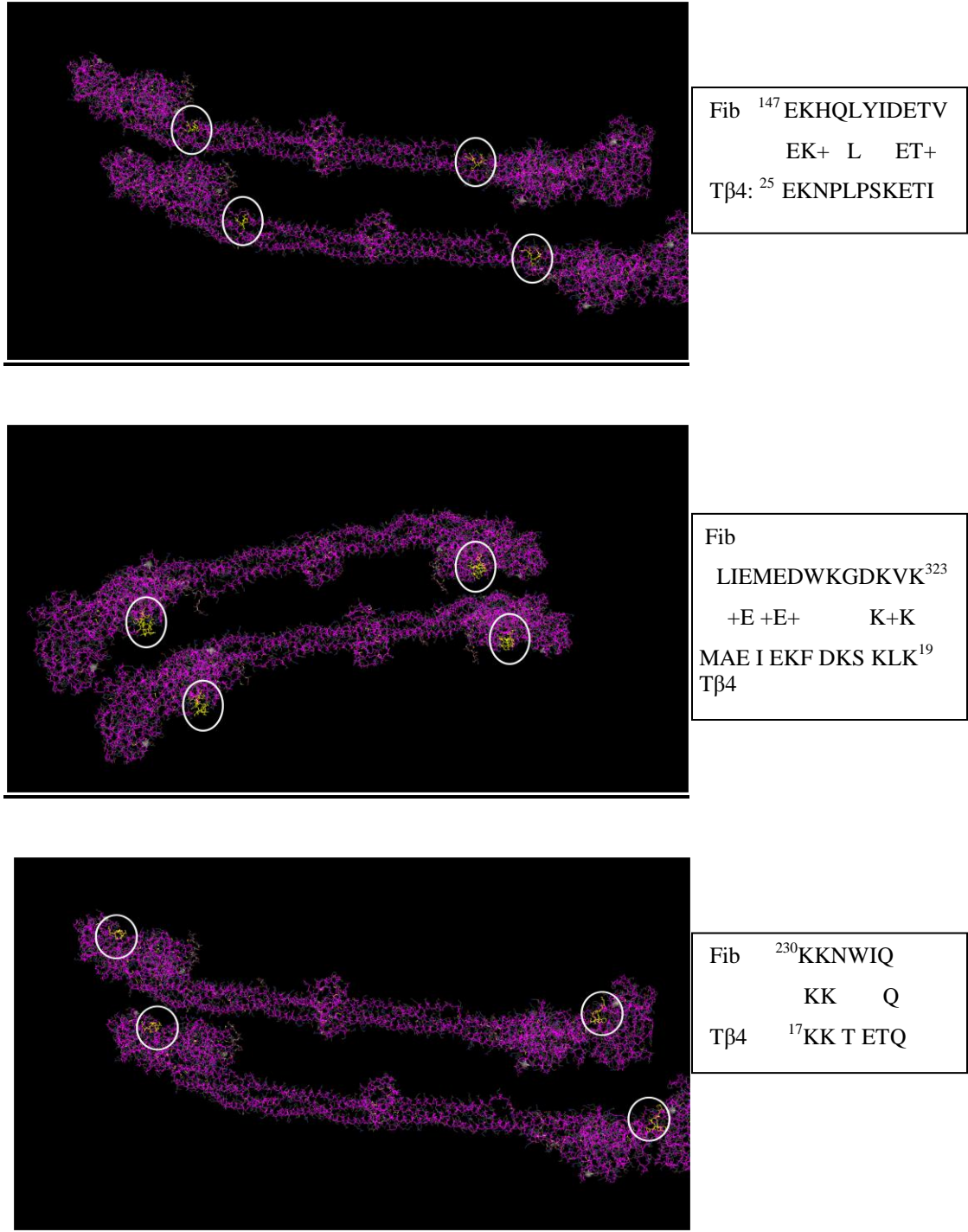


Figure 4-1 Consensus sequences between fibrinogen and Tβ4 that may produce a binding site for Tβ4 on fibrinogen (images acquired from NCBI MMDB (83))

Chapter 4: Discussion

However, Huff et al in 2002 identified covalent bond formation between T β_4 and fibrinogen in the presence of tissue transglutaminase—which is co-released with T β_4 -- and suggest this as a mechanism to retain T β_4 near the site of release (61). Fixing T β_4 near the site of injury would theoretically make it available for participating in wound repair and healing, as the previously mentioned wound healing powers of T β_4 are well documented. It was further determined that the covalent bonds between fibrinogen and T β_4 were isopeptide bonds formed between reactive Gln and Lys residues in both the α and γ chains of fibrinogen, with the most likely incorporation within the A α 392-610 region of the fibrinogen α C domains (60). Makogonenko *et al.*, using concentrations higher than those utilized in this study, found that fibrinogen and T β_4 do not form non-covalent interactions in the absence of transglutaminase. Interestingly this is not completely contradictory to the results outlined in this thesis, as at concentrations above 30 $\mu\text{g/mL}$ the binding relationship between fibrinogen and T β_4 has been shown to trend back towards control levels; therefore it would be expected that at a concentration of 150 $\mu\text{g/mL}$, as used in the Makogonenko paper, the interaction between fibrinogen and T β_4 would be relatively low. When the T β_4 -fibrinogen binding curve is extrapolated to include a T β_4 concentration of 150 $\mu\text{g/mL}$, it becomes clear that at 150 $\mu\text{g/mL}$ concentration of T β_4 the relative binding occurring between T β_4 and fibrinogen is very close to the binding which occurs at very low (0.1 $\mu\text{g/mL}$) concentrations of T β_4 . Hence, the Makogonenko finding, suggesting that fibrinogen and T β_4 do not have noncovalent interactions, does not encompass the physiological range of T β_4 concentrations utilized in this study; furthermore, the most important T β_4 concentration range—around 5 $\mu\text{g/mL}$ —is not addressed at all. Incorporating these results and the theories expressed in the

Chapter 4: Discussion

Makogonenko and Huff papers, the following hypothesis has been developed. Upon initial platelet activation with thrombin $T\beta_4$ is released, associating with the platelet surface and potentiating platelet aggregation. At this point, since transglutaminase is co-released with $T\beta_4$, there is the potential for $T\beta_4$ bonds with fibrinogen being formed, in a concentration-dependent manner according to Makogonenko *et al.* Initially, the fibrinogen- $T\beta_4$ binding would be relatively low as the concentration of $T\beta_4$ would initially be low. At this time, $T\beta_4$ would be available to interact with the platelet surface, thereby potentiating platelet aggregation. As more platelets become activated and the thrombus grows, the $T\beta_4$ concentration would increase, with the proportion of the fibrinogen- $T\beta_4$ bound complex subsequently growing. Logically, the more clotting and platelet activation that occurs, the higher the $T\beta_4$ concentration, and the more $T\beta_4$ will be covalently bound to fibrinogen. Thus, as the thrombotic event proceeds the body has essentially created not only a matrix which can keep $T\beta_4$ at the site of injury for the purpose of wound repair, but a sink that in essence sequesters $T\beta_4$ from the platelet surface, removing the potentiation signal. By removing the potentiation signal, the body is preventing just one of the signals that would otherwise instigate an uncontrolled thrombotic event. Clearly $T\beta_4$ is not the only signaling molecule utilized for potentiation of the platelet aggregation reaction, so there are other components within the body that contribute to the down-regulation of the aggregation response after the bleeding at the site of injury has been stopped. However, it appears that the sequestration of $T\beta_4$ by tissue transglutaminase and fibrinogen may be one of those processes participating in this cascade. For diabetic patients, slightly elevated levels of $T\beta_4$ in platelets or in the blood could contribute to the increased propensity for thromboses, while high doses of $T\beta_4$

Chapter 4: Discussion

could represent a potential therapy for treatment of the thrombotic side effects of diabetes and other illnesses such as cardiovascular disease and atherosclerosis.

4.4 Future Directions

For future directions of this study, the most significant and important ones are as follows: further development of the flow cell chamber experimental method, and further investigation into $T\beta_4$ as a factor in thrombotic symptoms of diabetes, and possibly as a thrombotic inhibitor at high concentrations. To expand the experimental method of flow cell chamber experiments, the problems previously discussed in this study must be solved including the imaging of bound platelets, continuity of results from trial to trial and experiment to experiment, as well as implementing a technique to prevent the system from clogging and wasting valuable materials. As previously mentioned the most ideal solution to the problem of imaging bound platelets—while avoiding unbound platelets flowing above the PDMS surface—is developing a labeling technique that only allows platelets to become fluorescent once they have bound to fibrinogen on the PDMS surface. To prevent the system from clogging, it might be effective to use a larger blood source to prevent blood and the platelets therein from continuously being exposed to the stresses within the tube system, as in the current experimental set up. With a larger blood volume to pull from, platelets and red blood cells returning to the blood pool would theoretically have a longer wait time before being sucked back into the tube system, thus administering less stress per cell.

Chapter 4: Discussion

Further investigation into $T\beta_4$ as a potential culprit in diabetic thromboses would require analysis of diabetic patients and their $T\beta_4$ levels, along with comparisons between the effects of $T\beta_4$ administration effects on diabetic platelets and compared to control platelets. Extending the study of $T\beta_4$ as an anti-thrombotic compound at high concentrations of administration would require studying the concept in animal models, inducing thrombotic events and measuring their severity at varying doses of $T\beta_4$. Furthermore, to confirm the location of the binding pocket on fibrinogen for $T\beta_4$, mutational studies would need to be conducted altering amino acids within the proposed binding pocket and measuring the effect of those mutations on $T\beta_4$ binding. Once the binding pocket for $T\beta_4$ could be verified, further research would be needed to elucidate the pathway including $T\beta_4$ as an effector in platelet aggregation, and how fibrinogen plays a role in this pathway.

REFERENCES

1. Bruce Goode, G. R. L. Model of the actin cytoskeleton, In *Power Point*, Brandeis University 415 South Street Waltham, MA 02454.
2. Patel, S. R., Hartwig, J. H., and Italiano, J. E., Jr. (2005) The biogenesis of platelets from megakaryocyte proplatelets, *J Clin Invest* 115, 3348-3354.
3. Monzen, S., Osuda, K., Miyazaki, Y., Hayashi, N., Takahashi, K., and Kashiwakura, I. (2009) Radiation sensitivities in the terminal stages of megakaryocytic maturation and platelet production, *Radiat Res* 172, 314-320.
4. Ravid, K., Lu, J., Zimmet, J. M., and Jones, M. R. (2002) Roads to polyploidy: the megakaryocyte example, *J Cell Physiol* 190, 7-20.
5. Behnke, O. (1968) An electron microscope study of the megakaryocyte of the rat bone marrow. I. The development of the demarcation membrane system and the platelet surface coat, *J Ultrastruct Res* 24, 412-433.
6. Zucker, M. B., and Nachmias, V. T. (1985) Platelet activation, *Arteriosclerosis* 5, 2-18.
7. Harrison, P., and Cramer, E. M. (1993) Platelet alpha-granules, *Blood Rev* 7, 52-62.
8. Coughlin, S. R. (2000) Thrombin signalling and protease-activated receptors, *Nature* 407, 258-264.
9. Vu, T. K., Hung, D. T., Wheaton, V. I., and Coughlin, S. R. (1991) Molecular cloning of a functional thrombin receptor reveals a novel proteolytic mechanism of receptor activation, *Cell* 64, 1057-1068.
10. Ginsberg, M. H., Partridge, A., and Shattil, S. J. (2005) Integrin regulation, *Curr Opin Cell Biol* 17, 509-516.
11. Takagi, J., Petre, B. M., Walz, T., and Springer, T. A. (2002) Global conformational rearrangements in integrin extracellular domains in outside-in and inside-out signaling, *Cell* 110, 599-511.
12. Xiao, T., Takagi, J., Collier, B. S., Wang, J. H., and Springer, T. A. (2004) Structural basis for allostery in integrins and binding to fibrinogen-mimetic therapeutics, *Nature* 432, 59-67.
13. Vinogradova, O., Velyvis, A., Velyviene, A., Hu, B., Haas, T., Plow, E., and Qin, J. (2002) A structural mechanism of integrin alpha(IIb)beta(3) "inside-out" activation as regulated by its cytoplasmic face, *Cell* 110, 587-597.
14. Walsh, G. M., Sheehan, D., Kinsella, A., Moran, N., and O'Neill, S. (2004) Redox modulation of integrin [correction of integin] alpha IIb beta 3 involves a novel allosteric regulation of its thiol isomerase activity, *Biochemistry* 43, 473-480.
15. Manickam, N., Sun, X., Hakala, K. W., Weintraub, S. T., and Essex, D. W. (2008) Thiols in the alphaIIbbeta3 integrin are necessary for platelet aggregation, *Br J Haematol* 142, 457-465.
16. Lahav, J., Wijnen, E. M., Hess, O., Hamaia, S. W., Griffiths, D., Makris, M., Knight, C. G., Essex, D. W., and Farndale, R. W. (2003) Enzymatically catalyzed

References

- disulfide exchange is required for platelet adhesion to collagen via integrin alpha2beta1, *Blood* 102, 2085-2092.
17. Mambula, S. S., Stevenson, M. A., Ogawa, K., and Calderwood, S. K. (2007) Mechanisms for Hsp70 secretion: crossing membranes without a leader, *Methods* 43, 168-175.
 18. Calderwood, S. K., Mambula, S. S., and Gray, P. J., Jr. (2007) Extracellular heat shock proteins in cell signaling and immunity, *Ann N Y Acad Sci* 1113, 28-39.
 19. Cederholm, A., Svenungsson, E., Stengel, D., Fei, G. Z., Pockley, A. G., Ninio, E., and Frostegard, J. (2004) Platelet-activating factor-acetylhydrolase and other novel risk and protective factors for cardiovascular disease in systemic lupus erythematosus, *Arthritis Rheum* 50, 2869-2876.
 20. Zhan, R., Leng, X., Liu, X., Wang, X., Gong, J., Yan, L., Wang, L., Wang, Y., and Qian, L. J. (2009) Heat shock protein 70 is secreted from endothelial cells by a non-classical pathway involving exosomes, *Biochem Biophys Res Commun* 387, 229-233.
 21. Gruden, G., Bruno, G., Chaturvedi, N., Burt, D., Pinach, S., Schalkwijk, C., Stehouwer, C. D., Witte, D. R., Fuller, J. H., and Cavallo-Perin, P. (2009) ANTI-HSP60 and ANTI-HSP70 antibody levels and micro/ macrovascular complications in type 1 diabetes: the EURODIAB Study, *J Intern Med*.
 22. Xiao, C., Chen, S., Yuan, M., Ding, F., Yang, D., Wang, R., Li, J., Tanguay, R. M., and Wu, T. (2004) Expression of the 60 kDa and 71 kDa heat shock proteins and presence of antibodies against the 71 kDa heat shock protein in pediatric patients with immune thrombocytopenic purpura, *BMC Blood Disord* 4, 1.
 23. Polanowska-Grabowska, R., Simon, C. G., Jr., Falchetto, R., Shabanowitz, J., Hunt, D. F., and Gear, A. R. (1997) Platelet adhesion to collagen under flow causes dissociation of a phosphoprotein complex of heat-shock proteins and protein phosphatase 1, *Blood* 90, 1516-1526.
 24. Xiao, R., Lundstrom-Ljung, J., Holmgren, A., and Gilbert, H. F. (2005) Catalysis of thiol/disulfide exchange. Glutaredoxin 1 and protein-disulfide isomerase use different mechanisms to enhance oxidase and reductase activities, *J Biol Chem* 280, 21099-21106.
 25. Noiva, R. (1994) Enzymatic catalysis of disulfide formation, *Protein Expr Purif* 5, 1-13.
 26. Cabrera, M., Muniz, M., Hidalgo, J., Vega, L., Martin, M. E., and Velasco, A. (2003) The retrieval function of the KDEL receptor requires PKA phosphorylation of its C-terminus, *Mol Biol Cell* 14, 4114-4125.
 27. Chen, K., Detwiler, T. C., and Essex, D. W. (1995) Characterization of protein disulphide isomerase released from activated platelets, *Br J Haematol* 90, 425-431.
 28. Pihlajaniemi, T., Helaakoski, T., Tasanen, K., Myllyla, R., Huhtala, M. L., Koivu, J., and Kivirikko, K. I. (1987) Molecular cloning of the beta-subunit of human prolyl 4-hydroxylase. This subunit and protein disulphide isomerase are products of the same gene, *EMBO J* 6, 643-649.
 29. Wetterau, J. R., Combs, K. A., Spinner, S. N., and Joiner, B. J. (1990) Protein disulfide isomerase is a component of the microsomal triglyceride transfer protein complex, *J Biol Chem* 265, 9800-9807.

References

30. Kemmink, J., Darby, N. J., Dijkstra, K., Nilges, M., and Creighton, T. E. (1996) Structure determination of the N-terminal thioredoxin-like domain of protein disulfide isomerase using multidimensional heteronuclear $^{13}\text{C}/^{15}\text{N}$ NMR spectroscopy, *Biochemistry* **35**, 7684-7691.
31. Edman, J. C., Ellis, L., Blacher, R. W., Roth, R. A., and Rutter, W. J. (1985) Sequence of protein disulphide isomerase and implications of its relationship to thioredoxin, *Nature* **317**, 267-270.
32. Hatahet, F., and Ruddock, L. W. (2007) Substrate recognition by the protein disulfide isomerases, *FEBS J* **274**, 5223-5234.
33. Nguyen, V. D., Wallis, K., Howard, M. J., Haapalainen, A. M., Salo, K. E., Saaranen, M. J., Sidhu, A., Wierenga, R. K., Freedman, R. B., Ruddock, L. W., and Williamson, R. A. (2008) Alternative conformations of the x region of human protein disulphide-isomerase modulate exposure of the substrate binding b' domain, *J Mol Biol* **383**, 1144-1155.
34. Tian, G., Kober, F. X., Lewandrowski, U., Sickmann, A., Lennarz, W. J., and Schindelin, H. (2008) The catalytic activity of protein-disulfide isomerase requires a conformationally flexible molecule, *J Biol Chem* **283**, 33630-33640.
35. Tian, G., Xiang, S., Noiva, R., Lennarz, W. J., and Schindelin, H. (2006) The crystal structure of yeast protein disulfide isomerase suggests cooperativity between its active sites, *Cell* **124**, 61-73.
36. Kozlov, G., Maattanen, P., Schrag, J. D., Pollock, S., Cygler, M., Nagar, B., Thomas, D. Y., and Gehring, K. (2006) Crystal structure of the bb' domains of the protein disulfide isomerase ERp57, *Structure* **14**, 1331-1339.
37. Hatahet, F., and Ruddock, L. W. (2009) Protein Disulfide Isomerase: A Critical Evaluation of Its Function in Disulfide Bond Formation, *Antioxid Redox Signal*.
38. Koivunen, P., Pirneskoski, A., Karvonen, P., Ljung, J., Helaakoski, T., Notbohm, H., and Kivirikko, K. I. (1999) The acidic C-terminal domain of protein disulfide isomerase is not critical for the enzyme subunit function or for the chaperone or disulfide isomerase activities of the polypeptide, *EMBO J* **18**, 65-74.
39. Raturi, A., and Mutus, B. (2007) Characterization of redox state and reductase activity of protein disulfide isomerase under different redox environments using a sensitive fluorescent assay, *Free Radic Biol Med* **43**, 62-70.
40. Mezghrani, A., Fassio, A., Benham, A., Simmen, T., Braakman, I., and Sitia, R. (2001) Manipulation of oxidative protein folding and PDI redox state in mammalian cells, *EMBO J* **20**, 6288-6296.
41. Miersch, S., Sliskovic, I., Raturi, A., and Mutus, B. (2007) Antioxidant and antiplatelet effects of rosuvastatin in a hamster model of prediabetes, *Free Radic Biol Med* **42**, 270-279.
42. Lahav, J., Gofer-Dadosh, N., Luboshitz, J., Hess, O., and Shaklai, M. (2000) Protein disulfide isomerase mediates integrin-dependent adhesion, *FEBS Lett* **475**, 89-92.
43. Gofer-Dadosh, N., Klepfish, A., Schmilowitz, H., Shaklai, M., and Lahav, J. (1997) Affinity modulation in platelet alpha 2 beta 1 following ligand binding, *Biochem Biophys Res Commun* **232**, 724-727.
44. Yan, B., and Smith, J. W. (2000) A redox site involved in integrin activation, *J Biol Chem* **275**, 39964-39972.

References

45. Mor-Cohen, R., Rosenberg, N., Landau, M., Lahav, J., and Seligsohn, U. (2008) Specific cysteines in beta3 are involved in disulfide bond exchange-dependent and -independent activation of alphaIIb beta3, *J Biol Chem* 283, 19235-19244.
46. Yan, B., and Smith, J. W. (2001) Mechanism of integrin activation by disulfide bond reduction, *Biochemistry* 40, 8861-8867.
47. Essex, D. W., and Li, M. (1999) Protein disulphide isomerase mediates platelet aggregation and secretion, *Br J Haematol* 104, 448-454.
48. Kivirikko, K. I., and Myllyharju, J. (1998) Prolyl 4-hydroxylases and their protein disulfide isomerase subunit, *Matrix Biol* 16, 357-368.
49. Lamberg, A., Jauhiainen, M., Metso, J., Ehnholm, C., Shoulders, C., Scott, J., Pihlajaniemi, T., and Kivirikko, K. I. (1996) The role of protein disulphide isomerase in the microsomal triacylglycerol transfer protein does not reside in its isomerase activity, *Biochem J* 315 (Pt 2), 533-536.
50. Zai, A., Rudd, M. A., Scribner, A. W., and Loscalzo, J. (1999) Cell-surface protein disulfide isomerase catalyzes transnitrosation and regulates intracellular transfer of nitric oxide, *J Clin Invest* 103, 393-399.
51. Remijn, J. A., Wu, Y. P., Jeninga, E. H., MJ, I. J., van Willigen, G., de Groot, P. G., Sixma, J. J., Nurden, A. T., and Nurden, P. (2002) Role of ADP receptor P2Y(12) in platelet adhesion and thrombus formation in flowing blood, *Arterioscler Thromb Vasc Biol* 22, 686-691.
52. Ingerman-Wojenski, C., Smith, J. B., and Silver, M. J. (1983) Evaluation of electrical aggregometry: comparison with optical aggregometry, secretion of ATP, and accumulation of radiolabeled platelets, *J Lab Clin Med* 101, 44-52.
53. Kundu, S. K., Heilmann, E. J., Sio, R., Garcia, C., Davidson, R. M., and Ostgaard, R. A. (1995) Description of an in vitro platelet function analyzer--PFA-100, *Semin Thromb Hemost* 21 Suppl 2, 106-112.
54. Rand, M. L., Leung, R., and Packham, M. A. (2003) Platelet function assays, *Transfus Apher Sci* 28, 307-317.
55. Low, T. L., Hu, S. K., and Goldstein, A. L. (1981) Complete amino acid sequence of bovine thymosin beta 4: a thymic hormone that induces terminal deoxynucleotidyl transferase activity in thymocyte populations, *Proc Natl Acad Sci U S A* 78, 1162-1166.
56. Safer, D., Elzinga, M., and Nachmias, V. T. (1991) Thymosin beta 4 and Fx, an actin-sequestering peptide, are indistinguishable, *J Biol Chem* 266, 4029-4032.
57. Hannappel, E., and van Kampen, M. (1987) Determination of thymosin beta 4 in human blood cells and serum, *J Chromatogr* 397, 279-285.
58. Malinda, K. M., Sidhu, G. S., Mani, H., Banaudha, K., Maheshwari, R. K., Goldstein, A. L., and Kleinman, H. K. (1999) Thymosin beta4 accelerates wound healing, *J Invest Dermatol* 113, 364-368.
59. Nachmias, V. T., Cassimeris, L., Golla, R., and Safer, D. (1993) Thymosin beta 4 (T beta 4) in activated platelets, *Eur J Cell Biol* 61, 314-320.
60. Makogonenko, E., Goldstein, A. L., Bishop, P. D., and Medved, L. (2004) Factor XIIIa incorporates thymosin beta4 preferentially into the fibrin(ogen) alphaC-domains, *Biochemistry* 43, 10748-10756.

References

61. Huff, T., Otto, A. M., Muller, C. S., Meier, M., and Hannappel, E. (2002) Thymosin beta4 is released from human blood platelets and attached by factor XIIIa (transglutaminase) to fibrin and collagen, *FASEB J* 16, 691-696.
62. Gondo, H., Kudo, J., White, J. W., Barr, C., Selvanayagam, P., and Saunders, G. F. (1987) Differential expression of the human thymosin-beta 4 gene in lymphocytes, macrophages, and granulocytes, *J Immunol* 139, 3840-3848.
63. Sosne, G., Qiu, P., and Kurpakus-Wheatler, M. (2007) Thymosin beta 4: A novel corneal wound healing and anti-inflammatory agent, *Clin Ophthalmol* 1, 201-207.
64. Czisch, M., Schleicher, M., Horger, S., Voelter, W., and Holak, T. A. (1993) Conformation of thymosin beta 4 in water determined by NMR spectroscopy, *Eur J Biochem* 218, 335-344.
65. Safer, D., Sosnick, T. R., and Elzinga, M. (1997) Thymosin beta 4 binds actin in an extended conformation and contacts both the barbed and pointed ends, *Biochemistry* 36, 5806-5816.
66. Carlier, M. F., Hertzog, M., Didry, D., Renault, L., Cantrelle, F. X., van Heijenoort, C., Knossow, M., and Guittet, E. (2007) Structure, function, and evolution of the beta-thymosin/WH2 (WASP-Homology2) actin-binding module, *Ann N Y Acad Sci* 1112, 67-75.
67. Irobi, E., Aguda, A. H., Larsson, M., Guerin, C., Yin, H. L., Burtnick, L. D., Blanchoin, L., and Robinson, R. C. (2004) Structural basis of actin sequestration by thymosin-beta4: implications for WH2 proteins, *EMBO J* 23, 3599-3608.
68. Vancompernelle, K., Goethals, M., Huet, C., Louvard, D., and Vandekerckhove, J. (1992) G- to F-actin modulation by a single amino acid substitution in the actin binding site of actobindin and thymosin beta 4, *EMBO J* 11, 4739-4746.
69. Yarmola, E. G., Klimenko, E. S., Fujita, G., and Bubb, M. R. (2007) Thymosin beta4: actin regulation and more, *Ann N Y Acad Sci* 1112, 76-85.
70. Malinda, K. M., Goldstein, A. L., and Kleinman, H. K. (1997) Thymosin beta 4 stimulates directional migration of human umbilical vein endothelial cells, *FASEB J* 11, 474-481.
71. Carpinterio, P., Anadon, R., del Amo, F. F., and Gomez-Marquez, J. (1995) The thymosin beta 4 gene is strongly activated in neural tissues during early postimplantation mouse development, *Neurosci Lett* 184, 63-66.
72. Shenkman, B., Einav, Y., Salomon, O., Varon, D., and Savion, N. (2008) Testing agonist-induced platelet aggregation by the Impact-R [Cone and platelet) analyzer (CPA)], *Platelets* 19, 440-446.
73. Jacobs, R. M., Boyce, J. T., and Kociba, G. J. (1986) Flow cytometric and radioisotopic determinations of platelet survival time in normal cats and feline leukemia virus-infected cats, *Cytometry* 7, 64-69.
74. Dale, G. L., Remenyi, G., and Friese, P. (2009) Tetraspanin CD9 is required for microparticle release from coated-platelets, *Platelets*, 1-6.
75. Baker, G. R., Sullam, P. M., and Levin, J. (1997) A simple, fluorescent method to internally label platelets suitable for physiological measurements, *Am J Hematol* 56, 17-25.
76. Barhoumi, R., Bowen, J. A., Stein, L. S., Echols, J., and Burghardt, R. C. (1993) Concurrent analysis of intracellular glutathione content and gap junctional intercellular communication, *Cytometry* 14, 747-756.

References

77. Probes, I. M. (2008) CellTracker™ Probes for Long-Term Tracing of Living Cells, (Invitrogen, Ed.).
78. Ball, C., Vijayan, K. V., Nguyen, T., Anthony, K., Bray, P. F., Essex, D. W., and Dong, J. F. (2008) Glutathione regulates integrin alpha(IIb)beta(3)-mediated cell adhesion under flow conditions, *Thromb Haemost* 100, 857-863.
79. Bennett, J. S., Berger, B. W., and Billings, P. C. (2009) The structure and function of platelet integrins, *J Thromb Haemost* 7 Suppl 1, 200-205.
80. Voss, B., McLaughlin, J. N., Holinstat, M., Zent, R., and Hamm, H. E. (2007) PAR1, but not PAR4, activates human platelets through a Gi/o/phosphoinositide-3 kinase signaling axis, *Mol Pharmacol* 71, 1399-1406.
81. Essex, D. W., and Li, M. (1999) A polyclonal antibody to protein disulfide isomerase induces platelet aggregation and secretion, *Thromb Res* 96, 445-450.
82. Wang, S. S., Wang, B. S., Chang, J. K., Low, T. L., and Goldstein, A. L. (1981) Synthesis of thymosin beta 4, *Int J Pept Protein Res* 18, 413-415.
83. Kollman, J. M., Pandi, L., Sawaya, M. R., Riley, M., and Doolittle, R. F. (2009) Crystal structure of human fibrinogen, *Biochemistry* 48, 3877-3886.

VITA AUCTORIS

NAME Rebecca Catherine Heeney
PLACE OF BIRTH London, Ontario 1983
EDUCATION Glendale High School, Tillsonburg Ontario
1998-2002
University of Western Ontario, London Ontario
2002-2007 BMSc